BOEING

HIGH SPEED RESEARCH

Airframe Materials & Structures - 4.2
Aeroelasticity - 4.2.6

Multi-Year Summary Report
For Calendar Years 1995 - 1999

Prepared for
NASA AERONAUTICS AND SPACE ADMINISTRATION
LANGLEY RESEARCH CENTER
HAMPTON, VIRGINIA 23665-5225

Under Contract NAS1-20220

September 30, 1999
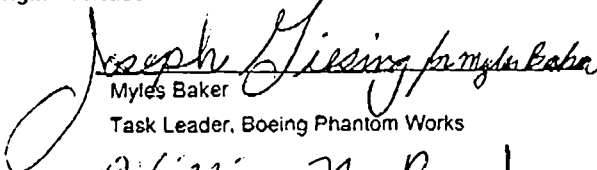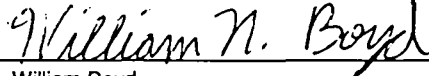
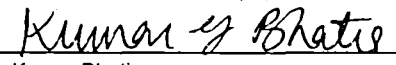## BOEING COMMERCIAL AIRPLANE GROUP

BOEING PHANTOM WORKS

Document Information

Document Type	Original Release Date	Contract Number (if required)
Formal	September 30, 1999	NAS1-20220

Preparing Organization (if different from owning organization)	Hardware and Software Used
	IBM PC Microsoft Word 97 SR2

Notes and Limitations (optional)

Signatures for original release

		Org. Number	Date
EDITED BY:	Myles Baker Task Leader, Boeing Phantom Works	CG-01X2	9-30-99
EDITED BY:	William Boyd Task Leader, Boeing Commercial Airplane Grp	B-YB80	9/30/99
EDITED BY:	Robert Scott Task Leader, NASA Langley Research Center	Aeroelasticity Br	9/50/99
APPROVAL:	Kumar Bhatia Task Integrator	B-YB00	9-30-1999
APPROVAL:	Joseph Giesing ITD Member, Boeing Phantom Works	CG-02LB	9-30-99
APPROVAL:	Steve Precup Manager, Boeing Commercial Airplane Grp	B-YB80	9/30/99
APPROVAL:	Peter Rimbos HSCT-AT AM&S Principal Investigator	B-YG11	9/30/99

ACKNOWLEDGEMENTS

Table of Contents

List of Figures

List of Tables

1. Executive Summary

The Aeroelasticity Task is intended to provide demonstrated technology readiness to predict and improve flutter characteristics of an HSCT configuration. This requires aerodynamic codes that are applicable to the wide range of flight regimes in which the HSCT will operate, and are suitable to provide the higher fidelity required for evaluation of aeroservoelastic coupling effects. Prediction of these characteristics will result in reduced airplane weight and risk associated with a highly flexible, low-aspect ratio supersonic airplane with narrow fuselage, relatively thin wings, and heavy engines.

This Task is subdivided into three subtasks. The first subtask includes the design, fabrication, and testing of wind-tunnel models suitable to provide an experimental database relevant to HSCT configurations. The second subtask includes validation of candidate unsteady aerodynamic codes, applicable in the Mach and frequency ranges of interest for the HSCT, through analysis test correlation with the test data. The third subtask includes efforts to develop and enhance these codes for application to HSCT configurations.

The wind tunnel models designed and constructed during this program furnished data which were useful for the analysis test correlation work but there were shortcomings. There was initial uncertainty in the proper tunnel configuration for testing, there was a need for higher quality measured model geometry, and there was a need for better measured model displacements in the test data. One of the models exhibited changes in its dynamic characteristics during desting. Model design efforts were hampered by a need for more and earlier analysis support and better knowledge of material properties.

Success of the analysis test correlation work was somewhat muted by the uncertainties in the wind tunnel model data. The planned extent of the test data was not achieved, partly due to the delays in the model design and fabrication which could not be extended due to termination of the HSR program.

1.1 Wind Tunnel Models

1.1.1 Baseline I wind tunnel models database

Two semi-span wind tunnel models were designed, built, and tested at NASA LaRC. The objective was to provide data relevant to critical aeroelastic phenomena of a representative HSCT configuration for analysis/test correlation work. Both models were based on the Boeing Reference HSCT Configuration (Reference H) wing in $1/12^{th}$ scale and included a simplified fuselage shell. Test results were provided for the purpose of furthering the analytical capabilities of predicting flutter in the

preliminary design stages of an HSCT airplane program, affording insight into the applicability of different methodologies in different flight regimes. Test data was obtained for a fuselage/wing configuration and a fuselage/wing/nacelles/diverter configuration, using air and a heavy gas medium (Freon R12).

The Rigid Semispan (RSM) wind tunnel flutter model was developed primarily to provide steady and unsteady aerodynamic data. Wing construction was of graphite skins over foam core to maximize stiffness. The figure below shows an illustration of the key components and instrumentation for the RSM with the removable engine nacelles in place (fuselage section removed to show the wing rigid mounting beam). The wing and fuselage shell are instrumented with unsteady pressure transducers. The five-component instrumentation balance measures total force and moment components on the wing (isolated from fuselage contribution). Angle of attack is variable, and a hydraulically actuated flap can be harmonically excited to provide unsteady pressure data.

HIGH SPEED
HSR
REASEARCH

MODEL DETAILS

Rigid Semispan Model II

Layout and Instrumentation

O PRESSURE TRANSDUCERS (135)
  - 10%, 30%, 60% and 95% span
  - 20% chord at 20%, 45% and 75% span
  - upper and lower surface
□ ACCELEROMETERS (6-8)

Removable LE
Removable Tip Cap
Removable TE
Rigid-mounted Engines
TE Flaperon
Sealed gaps
Rigid Fuselage Fairing
Tunnel Wall
Balance
Pedestal
Rigid Mounting Beam
Tunnel Turntable

120 Fuselage ESP Pressure Ports (7 chordwise locations)
Fuselage Length = 18.39 ft.
Wing Span = 4.86 ft.
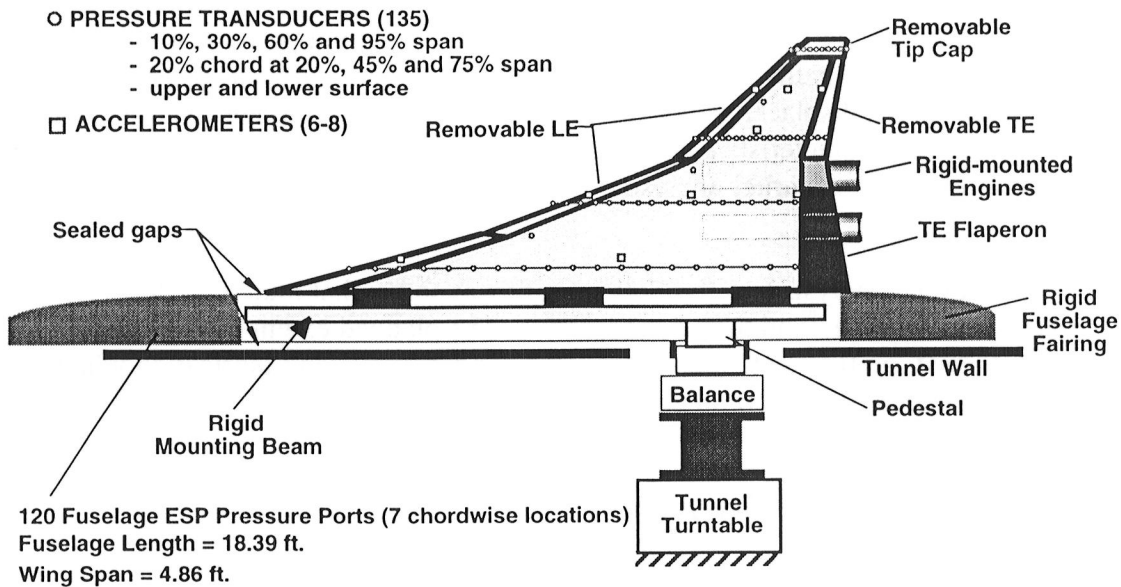
RSM II (Rebuilt)
Pretest - 7
D. Keller 3/5/96

Details of the Rigid Semispan Model (RSM)

The Flexible Semispan (FSM) is a highly instrumented aeroelastic wind tunnel model intended to produce steady and unsteady aeroelastic data for analysis test correlation

work. Model features were similar to those of the RSM, but wing construction was of fiberglass skins over foam core to allow a desired level of static and dynamic flexible deformation. Testing of the FSM was divided into two phases, an aerodynamic loads phase and a flutter-testing phase. During the aerodynamic loads phase, the pertinent acquired data consists of wing loads, surface pressures, and deflections for variation in angle of attack and for input of steady and oscillating flap deflections. During the flutter-testing phase of the test, dynamic data was acquired using flap oscillations to excite the model at subcritical conditions, and a flutter boundary was identified by observation of stability. There was some difficulty with changes in model dynamic characteristics during flutter testing. The FSM was destroyed due to flutter at Mach 0.98, but data had already been acquired for another hard flutter condition at Mach 0.945 as well as for multiple low damped response conditions near Mach 0.98.

1.1.2 Interim test program evaluation

A semispan wind-tunnel model for the purpose of measuring flutter at high angles of attack and with large control surface deflections had been envisioned during Aeroelasticity Task planning. It would be based on the Technology Concept Airplane (TCA). However, the TCA-FSM was assessed to be a lower priority than the other models in the program. The **TCA1-FSM requirement evaluation** milestone was identified to serve as a timely re-evaluation of the need for such a wind-tunnel model should program priorities change. This evaluation was completed by the Aeroelasticity ITD team via a recommendation that a separate model for high angle of attack studies not be built, but that the existing and planned models, particularly the RSM/PAPA and ASM, be used wherever possible to gather high angle of attack data.

1.1.3 Baseline II wind tunnel models database

Two additional test configurations were identified for the RSM, to provide both a one-degree-of-freedom and a two-degree-of-freedom testbed. For the first of these, the Pitch And Plunge Apparatus (PAPA) mount was used in order to provide steady and unsteady wind-tunnel test data including flutter data for an essentially two-degree-of-freedom dynamic system. An initial RSM/PAPA test was followed by a redesign of the mounting, fuselage shell, and mass ballast. The subsequent test produced unsteady model pressure, response, and stability measurements suitable for use in analysis/test correlation work. The measured Mach-Q flutter boundaries of the RSM/PAPA showed an interesting dependence of the flutter boundary on mean angle of attack, with the absence of flutter at positive angles.

For the second additional test configuration the RSM was to be mounted to the Oscillating Turn Table (OTT). The objective was to obtain steady and unsteady wind-tunnel test data, consisting primarily of model pressure measurements. Delays

in completion of the OTT apparatus kept this test from occurring before HSR contract termination. Nevertheless, industry supporting analysis was performed using CFL3D Euler and Euler/Navier-Stokes unsteady aerodynamics. This data can be used in future correlation efforts subsequent to the test.

1.1.4 ASE wind tunnel models database

Evaluation of the flying and ride qualities of the HSCT indicated a crucial need for structural mode control (SMC). This is a relatively high-risk area, and the need for ASE testing was highlighted for risk mitigation. In order to evaluate the aeroservoelastic characteristic and aeroelastic behavior of the Technology Concept Airplane (TCA), a full-span aeroservoelastic wind-tunnel model was planned. In order to improve the quality of data and reduce risk to this program three wind-tunnel models were to be built and tested: the Aeroservoelastic Semispan Model (ASM), the Rigid Fullspan Model (RFM), and the Aeroservoelastic Fullspan Model (AFM), collectively referred to as the ASE models.

The ASM, a semispan model which utilizes the TCA wing mounted on a flexible fuselage beam with horizontal tail, canard, and trailing edge flap as active controls, was the only one of the ASE models to be designed and constructed due to HSR contract termination. The ASM was designed to provide flutter and flutter sensitivity information, to measure frequency response functions relating control surface excitation to model response, and to be a testbed for investigating various control laws. Actual testing of the ASM was not performed before September 1999, forcing deletion of the ASM analysis/test correlation subtask.

A program milestone, **Preliminary FFM Specification,** was the focus of work to formulate specifications for and assist in the preliminary design of the ASE wind tunnel models. A Model Oversight Team, formed in January 1997, worked to develop a Specification Document for the ASE models which would define the models and provide a guide for potential vendors to follow in the design and fabrication of the models. Also, during August 1997, NASA requested that Boeing generate a Rough Order of Magnitude (ROM) estimate for the family of ASE wind tunnel models. The resulting ROM estimate exceeded the available budget, and was a factor in NASA's decision to design and fabricate the ASE models at NASA LaRC.

The milestone **TCA Parametric Flutter Analysis** was included in order to provide flutter sensitivity data with which to support scaling and design of the ASE wind tunnel models. Finite element analysis work at Boeing based on the DITS structurally sized TCA was used to develop a recommended configuration for the ASE wind tunnel models. This recommended configuration (including FEM) was provided to the NASA design build team to support model design.

Model design/test support was provided by Boeing for the ASE wind tunnel models development work at NASA, particularly for the ASM. Boeing Material Technology (BMT) performed a series of laboratory tests from August 1998 into March 1999 on ASM materials samples provided by NASA. Boeing designed an idealized wing skin for the ASM out of a undirectional fiberglass prepreg material at NASA's request. Boeing also determined an idealized fuselage stiffness distribution that would produce the desired flutter boundary. Boeing performed as well a series of analyses to determine the size and location of the wing-to-fuselage mounting brackets. Also studied were nacelle/pylon stiffness and mounting of the flexible fuselage. Other miscellaneous support activities included definition of a pressure tap layout for the ASM wing, investigation of leading edge flow separation on the outboard wing of the TCA configuration, definition of a mass panel breakdown of the ASM wing, and numerous flutter sensitivity analyses.

Boeing personnel participated in the ASM model critical design review held April 28-30, 1999 at NASA Langley Research Center. The Review consisted of presentations by the NASA model design team and a presentation by Boeing describing scaling and FEM analysis of the model wing design.

1.2 Analysis/Test Correlation

1.2.1 Code assessment I

Based on analysis/test correlation with data obtained through the **Baseline I semispan models wind-tunnel test database**, a preliminary assessment of several analysis codes was made with regard to analyses accuracy in predicting loads and flutter for HSCT configurations. The focus of this assessment was the CFD codes PANAIR, TRANAIR, and CFL3D. Some comparisons using the doublet lattice linear lifting surface method were also made.

PANAIR is a higher-order panel method which solves the linearized potential-flow boundary-value problem. It cannot represent viscous flow effects, thus it is generally limited to subsonic and supersonic (not transonic) flight regimes, but the wing, empennage, body, and nacelle geometry is accurately represented. TRANAIR solves the full potential flow equations with a coupled boundary layer and is widely used at Boeing. It is suitable for modeling subsonic, transonic, and supersonic flows; however, it cannot accurately predict flows dominated by viscous effects (other than boundary layer), nor can it accurately predict flows dominated by *strong* (non-isentropic) transonic flow effects. CFL3D, the paramount code being assessed, is a Reynolds-Averaged thin-layer Navier-Stokes flow solver for structured multi-block grids developed at NASA Langley Research Center and enhanced by Boeing to add aeroelastic analysis capability. CFL3D is applicable across the Mach range of interest and is particularly well suited for modeling viscous dominated flows with

leading-edge flow separations, and is best suited of these three codes to model the physics of the nonlinear flow phenomena that may impact flutter.

The following table summarizes the steady-flow analysis/test correlation results for the RSM (clean-wing configuration) for Mach range for 0.70 to 1.15 and angle of attack limited to 0 and 2 degrees.

Codes	Mach Number Range		
	0.7 to 0.9	0.9 to 1.05	1.05 to 1.15
Linear Theory	✔+	✔-	✔-
PANAIR (A502)	✔+	✔-	✔-
TRANAIR (w/ Boundary Layer)	✔+	✔	✔+
CFL3D (Navier-Stokes)	✔+	✔+	✔+

✔+ Good; ✔ Adequate; ✔- Poor

CFL3D demonstrated good overall correlation for the limited angles of attacks correlated, provided that viscous effects are modeled in the transonic flow range. TRANAIR with a coupled boundary layer solution provided satisfactory overall correlation for the limited angles of attack. Both PANAIR and Linear Theory demonstrated good correlation for the subsonic conditions, but showed poor correlation in the transonic and low supersonic range.

Unsteady-flow correlation for the RSM was limited to wing pressure data for flap oscillations at Mach 0.80 and 2 degrees angle of attack. Overall, the analytical codes - PANAIR, TRANAIR, and CFL3D - predicted the magnitude of the unsteady pressure to be higher than the measured data.

The FSM correlation was clouded by uncertainties in the wind tunnel model definition and test data, which affects validity of the finite element models used for aeroelastic analysis. In spite of these deficiencies, there was good correlation with wing force, wing moment, and pressure data at subsonic and supersonic conditions. The correlation was not completely satisfactory because of discrepancies with measured wing twist and deflection data. Flutter analysis produced encouraging correlation with the limited flutter data for the FSM, in spite of uncertainties in the test configuration. Nonlinear flutter analysis in CDFL3D revealed a moderate instability at Mach 0.98 which was similar to responses observed in the test.

Testing of the RSM in the TDT demonstrated a strong influence of the configuration of the adjustable tunnel wall slots on the model test data. An analysis was conducted to investigate the wall interference effects in the TDT, with emphasis on how best to configure the tunnel for the ASE models tests. A CFD model which included the RSM configuration and the TDT test section walls with discrete contoured slots on

the floor, ceiling, and sidewalls was developed for TRANAIR, and sensitivity analyses was conducted. Results predicted a sensitivity of measured data to wall slot configuration, and recommendations were made for further analysis.

1.2.2 Code assessment II

An updated code assessment was made based on analysis/test correlation with data obtained through the **Baseline II semispan models wind-tunnel test database,** which contains results from the RSM-PAPA test. In addition, unsteady CFD predictions were made to support the RSM-OTT test, which was not performed during this contract work.

Analysis/test correlation of the RSM-PAPA configuration was very challenging since the configuration is very sensitive to small changes in the elastic axis/center of gravity/aerodynamic center positions. When the structural model was correlated to match experimental GVT frequencies and mode shapes and the aerodynamic model was modified to give the measured AC position, flutter correlation was fairly good.

An unsteady Euler analysis of the RSM-OTT was performed with the CFL3D.AE-BA code. The computed unsteady pressure results during the last cycle of sinusoidal pitching were post-processed using Fourier transformation to get magnitude and phase angle of $\Delta C_p/\Delta\alpha$. Results for oscillation at two frequency/amplitude cases for a range of angle of attack are provided to assist with test planning.

1.3 Nonlinear Flutter Analysis Methods

Under this subtask, nonlinear flutter analysis capability was developed and applied to the analysis of the wind tunnel models and the TCA configuration. The analysis capability consists of two main approaches. The first is a CFD based nonlinear analysis capability that can be used to analyze the most difficult cases encountered for free-flying aircraft. The second is an efficient, production-level flutter analysis and design process which uses nonlinear steady and unsteady wind tunnel or CFD data to correct or replace linear aerodynamics. These tools were applied in order to evaluate the importance of nonlinear aerodynamics in the significant flutter mechanisms, and to thereby reduce aeroelastic risk.

A verification of the flutter speed of the TCA baseline aircraft was performed using an aerodynamic theory that includes nonlinear effects determined using CFD data. Results for two angle-of-attack cases, the first an attached flow case (α=2.8°) and the second one being a leading-edge vortex dominated high alpha flow case (α=12.11°), gave aeroelastic frequencies which correlated fairly well with linear analyses while damping results varied significantly. The high angle-of-attack case does not show evidence of any new instabilities not seen with linear analysis, but existence of such

at other conditions is not precluded. A specific example is the B-1, for which a transonic instability could appear over a very small range of angle of attack.

Techniques were evaluated for implementation of an antisymmetric boundary condition for Euler/Navier-Stokes aeroelastic analysis in CFL3D. Analysis of an HSCT wing/body/tail configuration in yaw, which compared results for a half-model mesh with the new antisymmetric boundary conditions with results for a full model, was encouraging. Recommendations are made for further work to validate and extend this capability.

A new technique was developed in which system identification is used to easily extract modal frequencies and damping ratios from simulation time histories typically generated through CFD time-domain aeroelastic analysis. This is valuable to the flutter engineer as it provides the estimated aeroelastic roots and mode shapes with nonlinear effects included. The identified parameters can also be used to determine the variation in frequency and damping ratio as the airspeed is changed.

A technique called Local Equivalence has been used in the HSR Aeroelasticity task to develop corrections to linear frequency-domain unsteady aerodynamics based on nonlinear aerodynamic data from Euler/Navier-Stokes time-domain simulations. The method has been integrated into the aeroelastic solution sequences in MSC/NASTRAN. The resulting correction process has been successfully used for both static (i.e. loads) and dynamic (i.e. flutter) analysis on several configurations ranging from wind tunnel models to full scale aircraft.

2. Introduction

The design of an HSCT will be influenced by aeroelastic effects and structural dynamic response. This was particularly the case with the U.S. supersonic transport design. Program technical risks associated with aeroelasticity and structural dynamics involve the timely assessment of aeroelastic and structural dynamic effects, such as flutter and aeroservoelastic coupling, and timely accurate load prediction. In addition, ride and handling qualities have been identified as serious design problems for the HSCT. To mitigate these risks, the HSR Aeroelasticity task was formulated with the primary objectives: (1) to evaluate and develop procedures to predict and improve airplane aeroelastic and dynamic response characteristics, (2) to develop analyses and tests to validate unsteady aerodynamic loads and flutter predictions, (3) to evaluate and develop nonlinear analysis methods, and (4) to provide aeroservoelastic data for validating ASE modeling methods and control design techniques, as well as to provide experience in applying control laws to HSCT configurations.

2.1 Overall Objective

The Aeroelasticity Task is intended to provide demonstrated technology readiness to predict and improve flutter characteristics of an HSCT configuration. Prediction of such flutter characteristics will result in reduced airplane weight and risk associated with a highly flexible, low-aspect ratio supersonic airplane with relatively thin wings and heavy engines. Work in this task includes development and validation of unsteady aerodynamic codes applicable in the Mach and frequency ranges of interest for the HSCT. Such aerodynamic codes will be suitable to provide the higher fidelity required for evaluations of aeroservoelastic coupling effects. Work in this task also includes the design, fabrication, and testing of wind-tunnel models suitable to provide data for validation of the codes through analysis test correlation with the resulting data.

2.2 Approach

The first step in performing this work was to select candidate HSCT design concepts and appropriate aerodynamic/aeroelastic codes and analysis methods. Next, the HSCT design concepts were screened through aeroelastic and dynamic analyses to predict response characteristics so that appropriate conditions could be selected for evaluation via wind-tunnel testing. Under the original task planning, several wind-tunnel models of varying complexity were to be designed, fabricated and tested starting with a simple rigid semi-span model and ending with a flexible, full-span, model. In fact, three semispan models were designed and constructed under this task, and analysis test correlation was successfully performed for the initial two models.

Due to early termination of the HSR program in September 1999, the planned full-span rigid and flexible models were not built and tested.

The data obtained from the wind-tunnel tests were used for correlation with the results of computational aerodynamic analyses with the objective being to validate the codes and/or establish code enhancement requirements. Validation and enhancement of nonlinear computational methods and linear correction methods were performed as part of this task.

Task planning also included the development of aeroservoelastic simulation models to be validated using wind-tunnel data and for development of various control laws for demonstration during wind-tunnel testing. Most of this work was not accomplished before the September 1999 program termination.

2.3 Task Summary

The wind tunnel testing portion of this work encompassed the following models/ configurations: (1) the Rigid Semispan Model (RSM) mounted on a load-measuring balance, (2) the RSM mounted on a Pitch and Plunge Apparatus (PAPA), (3) the Flexible Semispan Model (FSM), and (4) the Aeroservoelastic Semispan Model (ASM). Testing of the ASM was not accomplished before the September 1999 termination of the HSR program; neither was planned testing of the RSM mounted on an Oscillating Turntable (OTT). Other HSR Aeroelasticity models also planned but not constructed were the Rigid Fullspan Model (RFM) on the sting and cables, and the Aeroservoelastic Fullspan Model (AFM) on the sting and cables.

Analysis/test correlation efforts were made for the RSM and FSM for the purpose of assessing the validity of the analysis methods used. In addition to these correlation tasks, a significant effort was also directed toward the development and validation of nonlinear flutter prediction methods. These tasks includes the application of TRANAIR, the use of and enhancements to the Euler/Navier-Stokes code CFL3D, and the development of empirical correction methods that can be applied to loads and flutter analysis as a way to benefit from the accuracy of nonlinear codes through the use of inexpensive linear codes.

2.4 Major Deliverables
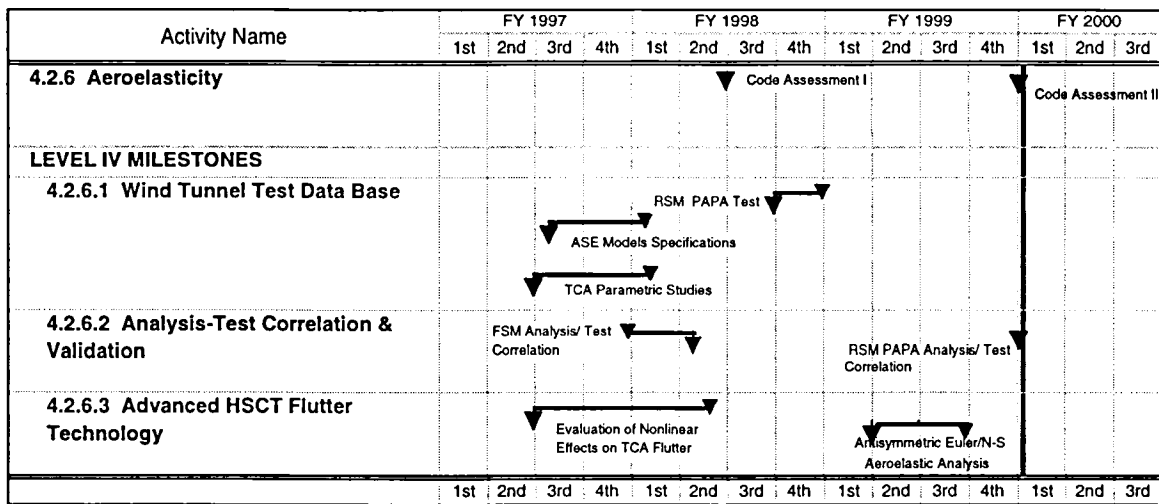
- Extensive unsteady aerodynamic and aeroservoelastic wind-tunnel database;

- Validated, calibrated, and corrected linear unsteady aerodynamic computational procedures and codes suitable for application to HSCT;

- Validated and enhanced nonlinear unsteady aerodynamic computational methods and codes suitable for application to HSCT;

- Aeroservoelastic testbed models for investigating and validating controls concepts.

2.5 Schedule

The following schedule highlights some of the industry milestones which occurred during the Aeroelasticity Task.

Activity Name	FY 1997				FY 1998				FY 1999				FY 2000		
	1st	2nd	3rd	4th	1st	2nd	3rd	4th	1st	2nd	3rd	4th	1st	2nd	3rd
4.2.6 Aeroelasticity							▼ Code Assessment I						▼ Code Assessment II		
LEVEL IV MILESTONES															
4.2.6.1 Wind Tunnel Test Data Base					RSM PAPA Test ▼→▼										
			▼→ ASE Models Specifications												
			▼→ TCA Parametric Studies												
4.2.6.2 Analysis-Test Correlation & Validation	FSM Analysis/ Test Correlation ▼→ ▼								RSM PAPA Analysis/ Test ▼ Correlation						
4.2.6.3 Advanced HSCT Flutter Technology	▼→▼ Evaluation of Nonlinear Effects on TCA Flutter								Antisymmetric Euler/N-S ▼→ ▼ Aeroelastic Analysis						
	1st	2nd	3rd	4th	1st	2nd	3rd	4th	1st	2nd	3rd	4th	1st	2nd	3rd

2.6 Level 3 and 4 Milestones

The following table lists the program level 3 and 4 milestones including those for NASA as well as industry. Work described in Sections 3-5 is organized by Work Breakdown Structure (WBS), which is identified as a column of the table below. Work performed to support milestones within WBS 4.2.6.1 (Wind Tunnel Test Data Base) is described in Section 3. Work that supports milestones under WBS 4.2.6.2 (Analysis-Test Correlation and Validation) is described in Section 4. Work performed to support milestones within WBS 4.2.6.3 (Advanced HSCT Flutter Technology) is described in Section 5.

WBS	NAME	PLANNED FINISH	ACTUAL FINISH
4.2.6.1	INTERIM TEST PROGRAM EVALUATION	28-Mar-97	30-Sep-97
4.2.6.1	BASELINE I S/S MODELS WIND TUNNEL TEST DATABASE	30-Aug-96	30-Aug-96
4.2.6.2	CODE ASSESSMENT I- ANALYSIS/TEST CORRELATION	31-Mar-98	31-Mar-98
4.2.6.3	AEROELASTIC ANALYTICAL METHODS (LOADS & FLUTTER)	31-Mar-97	31-Mar-97
4.2.6	UPDATE METHODS, TEST RESULTS & CORRELATIONS-I	31-Mar-98	31-Mar-98
4.2.6.99	PCD2 DRAFT	29-Dec-95	29-Dec-95
4.2.6.99	TASK BUDGETARY ESTIMATE	29-Jan-96	29-Jan-96
4.2.6.1	TCA1-FSM REQUIREMENT EVALUATION	31-Mar-97	29-Aug-97
4.2.6.99	PCD III DRAFT	1-Sep-98	20-Oct-98
4.2.6.1	RSM BALANCE TEST (FLAP & NO FLAP)		5-Apr-96
4.2.6.1	FSM TEST (GVT & WIND TUNNEL)		6-May-96
4.2.6.1	RSM DESIGN & FABRICATION		4-Mar-96
4.2.6.1	FFM/ASE SPECIFICATIONS COMPLETE	29-Apr-97	30-Oct-97
4.2.6.1	FFM SPEC DEVELOPMENT		30-Oct-97
4.2.6.1	RSM BALANCE TEST COMPLETE	29-Mar-96	5-Apr-96
4.2.6.1	FLEXIBLE SEMISPAN MODEL TEST COMPLETE	30-Apr-96	6-May-96
4.2.6.1	TCA1-FSM REQUIREMENT EVALUATION	27-Mar-97	29-Aug-97
4.2.6.1	RSM PAPA TEST COMPLETE	29-Jun-98	30-Sep-98
4.2.6.1	MODIFY RSM PAPA IF NEEDED		19-Dec-97
4.2.6.1	DEVELOP FEM BASED ON FSM MODEL		20-Dec-96
4.2.6.1	DELIVER RSM TEST RESULTS	28-Jun-96	28-Jun-96
4.2.6.1	DELIVER FSM TEST RESULTS	30-Aug-96	30-Aug-96

4.2.6.1	FFM DESIGN & FABRICATION		27-Apr-98
4.2.6.1	TCA PARAMETRIC STUDIES		7-Nov-97
4.2.6.1	DELIVER FFM PRELIMINARY SPECS	29-Mar-96	29-Mar-96
4.2.6.1	DELIVER PARAMETRIC FLUTTER ANALYSIS OF TCA	28-Mar-97	7-Nov-97
4.2.6.1	DELIVER RSM PAPA TEST RESULTS	30-Oct-98	30-Oct-98
4.2.6.1	DELIVER PRELIMINARY SPECS	29-Aug-96	29-Aug-96
4.2.6.1	DELIVER FFM PROPOSAL EVALUATION & DECISION	30-Dec-96	16-Jan-97
4.2.6.1	DELIVER FINAL FFM SPEC	29-Apr-97	30-Oct-97
4.2.6.1	TCA PARAMETRIC STUDIES	28-Mar-97	7-Nov-97
4.2.6.1	RSM/PAPA TEST RESULTS DELIVERABLE	30-Jun-98	30-Oct-98
4.2.6.1	ASE STATUS REPORT DELIVERABLE	31-Dec-98	31-Dec-98
4.2.6.2	RSM BALANCE ANALYSIS/TEST CORREL. (FLAP & NO FLAP)		30-Oct-96
4.2.6.2	FSM ANALYSIS/TEST CORRELATION		29-Sep-97
4.2.6.2	RSM ANALYSIS/TEST CORREL. (NO FLAP)		30-Oct-96
4.2.6.2	RSM BALANCE ANALYSIS/TEST CORR. (FLAP)		29-Sep-97
4.2.6.2	RSM BALANCE ANALYSIS/TEST CORRELATION COMPLETE	29-Aug-97	30-Sep-97
4.2.6.2	FSM ANALYSIS/TEST CORRELATION COMPLETE	30-Jan-98	30-Sep-97
4.2.6.2	DELIVER RSM ANALYSIS-TEST CORRELATION	30-Oct-96	31-Mar-97
4.2.6.2	DELIVER FSM ANALYSIS-TEST CORRELATION	30-Jun-97	20-Nov-97
4.2.6.2	DELIVER RSM ANALYSIS-TEST CORRELATION (FLAP-MDA)	28-Aug-97	15-Sep-97
4.2.6.2	DELIVER FFM CABLE-MOUNT STABILITY PRELIM ASSESSMENT	28-Aug-97	31-Oct-97
4.2.6.3	EMPIRICAL CORRECTIONS APPLIED TO LOADS & FLUTTER ANALYSIS	31-Oct-96	31-Oct-96
4.2.6.3	APPLICATION OF TRANAIR TO HSCT AERO. ANALYSIS	31-Dec-96	28-Mar-97
4.2.6.3	EVALUATE NONLINEAR EFFECTS ON TCA FLUTTER	31-Mar-97	20-Feb-98
4.2.6.3	EULER/N-S W/ DYNAMIC FLAP CAPABILITY	30-Jun-97	11-Jul-97
4.2.6.3	EMPIRICAL CORRECTIONS APPLIED TO LOADS & FLUTTER ANALYSIS		30-Oct-96

4.2.6.3	APPLICATION OF TRANAIR TO HSCT AERO ANALYSIS		28-Feb-97
4.2.6.3	EVALUATE NONLINEAR EFFECTS ON TCA FLUTTER		20-Feb-98
4.2.6.3	EULER/N-S W/ DYNAMIC FLAP CAPABILITY		11-Jul-97
4.2.6.3	DEL. EMPIRICAL CORRECTIONS TO STATIC LOADS & FLUTTER	30-Oct-96	15-Nov-96
4.2.6.3	DEL. APPLICATION OF TRANAIR TO HSCT AERO ANALYSIS	30-Dec-96	31-Mar-97
4.2.6.3	DEL. EVALUATION OF NONLINEAR EFFECTS ON TCA FLUTTER	30-Jun-97	13-Apr-98
4.2.6.3	DEL. TIME DOMAIN FLUTTER IDENTIFICATION TECHNIQUES	30-Dec-97	30-Jan-98
4.2.6.3	DEL. VALIDATED E/N-S CODE w/ DYNAMIC FLAP ANALYSIS	30-Jul-97	11-Jul-97
4.2.6.3	INVESTIGATE WIND TUNNEL INTERFERENCE IN TDT	30-Apr-98	30-Oct-98
4.2.6.3	ANTISYMMETRIC EULER/N-S AEROELASTIC ANALYSIS	31-Dec-98	31-Mar-99
4.2.6.3	UNSTEADY CORRECTED AERODYNAMICS FOR FSM	30-Apr-99	30-Jul-99
4.2.6.3	UPDATED EULER/NAVIER-STOKES AEROSERVOELASTIC CODE	31-Mar-99	31-Mar-99

3. Wind Tunnel Models

3.1 Baseline I Wind Tunnel Models Database

In order to reduce risks associated with aeroelastic impacts on the design of an HSR vehicle, a series of semi-span wind tunnel models/configurations were designed, built, and tested to provide insight into critical aeroelastic phenomena. Test results were provided for the purpose of furthering the analytical capabilities of predicting flutter in the preliminary design stages of an HSCT airplane program. These test results, through their use for analyses/test correlation, provide insight into the applicability of different methodologies in different flight regimes.

3.1.1 Rigid semispan model (RSM) balance test

The rigid semispan wind tunnel flutter model was developed primarily to provide steady and unsteady aerodynamic data which could support the analysis test work content of the HSR Aeroelasticity Task. . The wind tunnel model was designed and constructed at NASA LaRC and first tested on the balance system in the TDT in October 1994. Construction was of graphite skins over foam core to maximize stiffness. Figure 1 shows an illustration of the key components and instrumentation for the RSM with the removable engine nacelles in place (fuselage section removed to show the wing rigid mounting beam).

The wing is a $1/12^{th}$ scale model of the Boeing Reference HSCT Configuration (Reference H). The RSM wing was modified from the basic Reference H wing by increasing the thickness of the airfoil sections. The airfoil sections were scaled in the z-coordinate direction from the mean camber line to accommodate pressure transducers in the outboard wing. The RSM wing has a constant airfoil maximum thickness-to-chord ratio from the wing root to the wing tip of 4%.

The wing is instrumented with 131 high response unsteady pressure transducers at four semi-span locations. Six additional pressure transducers on the upper and lower surface are located at 20% chord and at 20%, 45%, and 75% semi-span. As shown in Figure 1, the RSM is outfitted with a hydraulically actuated flap. The flap is used to excite the flow field for unsteady flow measurements and is not representative of control systems of an actual HSCT configuration.

The wing rigid mounting beam is mounted to a five-component instrumentation balance which measures normal and axial forces and pitch, yaw, and roll moments. The wing (via the balance) is mounted to a jackscrew turntable providing a means for angle-of- attack adjustments.

The fuselage of the RSM has a rather blunt fore- and aft-body and was constructed to displace the wing away from, and outside of, the wind-tunnel wall boundary layer. It is not representative of an HSCT configuration. The fuselage is mounted to the turntable in such a way that the fuselage loads bypass the balance and the balance measures the wing-only loads. Not shown in Figure 1 are 119 Electronically Scanned Pressure (ESP) ports which are located at seven fuselage stations along the body. These ports allow steady pressure measurement on the fuselage.

A wind-tunnel test performed from 18 March to 4 April, 1996 in the TDT, reported in Reference 1, produced data which was used for the analysis test correlation work. This wind-tunnel test, designated as Test 520, was performed with the tunnel's east wall slots closed. (Earlier testing with the east wall slots open was judged to have produced erroneous results). Two configurations of the RSM were tested in the TDT - the fuselage/wing configuration and the fuselage/wing/nacelles/diverter configuration.

The wind-tunnel gas used during RSM Test 520 was Freon (R-12). Test data was acquired over a range of freestream Mach numbers from 0.70 to 1.15 at three levels of dynamic pressure: 100, 150, and 200 psf. For this range of Mach numbers and levels of dynamic pressure, steady wing and fuselage surface pressure distributions and steady wing aerodynamic loads were obtained at angles of attack ranging from -2° to +8°. The upper limit of the Mach number range was restricted by the tunnel operational limits and the angle-of-attack range was limited by the model strength. In addition to the angle-of-attack polar data, steady data was obtained for flap polars with flap angles ranging from -4° to +4°. Unsteady wing pressure data during harmonic flap oscillations was acquired for the clean wing configuration at $M_\infty=0.80$ and $\alpha=2°$. At these freestream conditions a sinusoidal flap oscillation was commanded about a zero degree mean flap deflection angle, $\delta_0=0°$. Data was acquired for several deflection amplitudes, $\delta_1=\pm2°$ and $\pm4°$, and for several frequencies, $f=1$, 2, and 5Hz. Reference 1 provides a more detailed description of the wind-tunnel data, illustrates the quality of the acquired data, and raises some issues with the data that deserve more attention.

Reference

1. Schuster, D. M., Rausch, R. D.; "Transonic Dynamics Tunnel Force and Pressure Data Acquired on the HSR Rigid Semispan Model"; Aeroelasticity Section Report LMES ASR 96-07; December, 1996.

HIGH SPEED
HSR
REASEARCH

MODEL DETAILS

Rigid Semispan
Model II

Layout and Instrumentation

O PRESSURE TRANSDUCERS (135)
 - 10%, 30%, 60% and 95% span
 - 20% chord at 20%, 45% and 75% span
 - upper and lower surface

□ ACCELEROMETERS (6-8)   Removable LE

Removable
Tip Cap

Removable TE

Rigid-mounted
Engines

TE Flaperon

Rigid
Fuselage
Fairing

Sealed gaps

Tunnel Wall

Balance   Pedestal

Rigid
Mounting Beam

Tunnel
Turntable

120 Fuselage ESP Pressure Ports (7 chordwise locations)
Fuselage Length = 18.39 ft.
Wing Span = 4.86 ft.
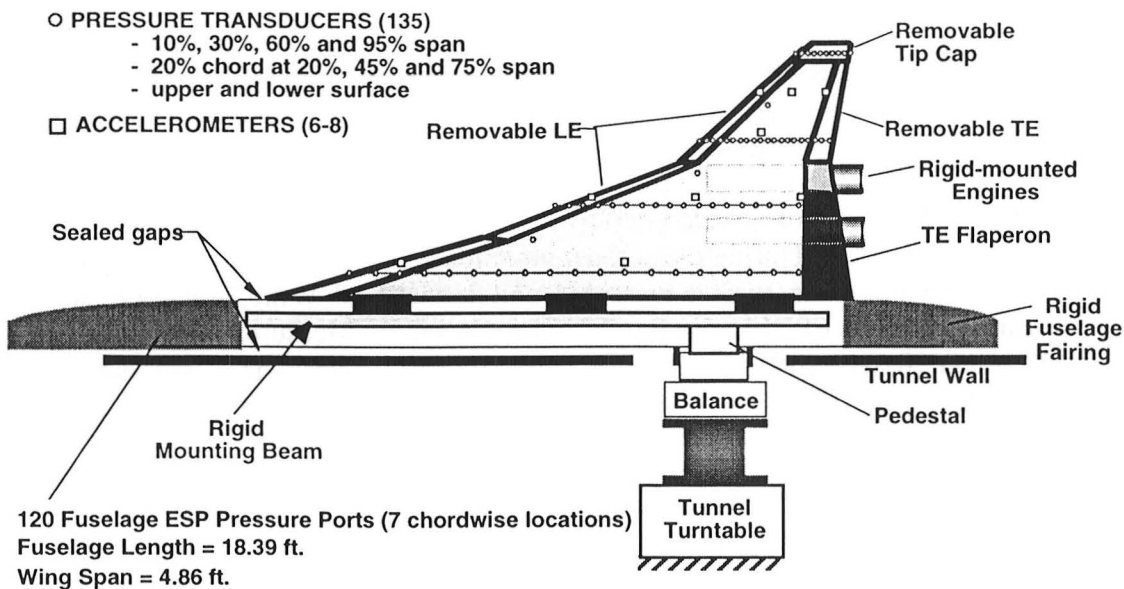
RSM II (Rebuilt)
Pretest - 7
D. Keller 3/5/96

Figure 1 Details of the Rigid Semispan Model (RSM).

3.1.2 Flexible semispan model (FSM) test

The FSM is a highly instrumented aeroelastic wind tunnel model intended to produce steady and unsteady aeroelastic data for the analysis test correlation work content of the Aeroelasticity Task. The FSM was tested in the NASA Langley Transonic Dynamics Tunnel (TDT), from April 4 to May 6, 1996, designated as Test 521. The FSM program was led by LaRC's Aeroelasticity Branch with participation by HSR partners (Boeing and McDonnell Douglas) and Lockheed Martin Engineering Sciences (LMES). A description of the development, analysis and testing of the FSM is given in Reference 2.

The FSM was the second of two correlation models tested in the TDT under the HSR Aeroelasticity effort. Three configurations of the FSM were tested - a clean wing, a wing with nacelles, and a flutter (clean wing) configuration (with a 2.5-lb. wing-tip trailing edge mass). Figure 2 shows an illustration of the key components and instrumentation for the FSM. The "flexible mounting beam" identified in the figure was in fact not used for testing, a "rigid" beam was used instead. Wing geometry,

instrumentation, and mounting system are similar to that of the RSM. Construction of the FSM was of fiberglass wing skins over a foam core. The skin layups were designed to give an "HSCT-like" flutter mechanism in the TDT operating envelope.

The wind tunnel medium was Freon (R-12). Test data was acquired over a Mach number range from 0.80 to 1.15. Over this range, aerodynamic data was obtained for an angle-of-attack range from -1° to +3°. The angle-of-attack range was limited by the aerodynamic loads the model could safely withstand. The upper limit of the Mach number range was restricted by the tunnel operational limit. Data was acquired at three levels of dynamic pressure: 100, 125, and 150 psf.

Testing of the FSM was divided into two phases, an aerodynamic loads phase and a flutter-testing phase. During the aerodynamic loads phase, the pertinent acquired data consists of wing loads, surface pressures, and deflections. Wing deflections were acquired using the EPIX Video Dynamic Displacement Measurement System (VDDMS). Sixteen EPIX targets were adhered to the lower surface, outboard portion, of the FSM wing. Using this system, displacements of the targets were obtained at the same time the loads and pressure data was obtained.

During the flutter-testing phase of the test, the five-component loads balance was replaced by a "dummy" balance to prevent its damage from anticipated dynamic loads. With the dummy balance, dynamic data was acquired using flap oscillations to excite the model. The magnitude of the response, due to the excitation, was a rough indication of the proximity to a flutter condition. Throughout the flutter-testing phase, the natural vibration frequencies of the model were checked as an indication of model integrity. Consequently, it was discovered that the modal frequencies of the first several modes were changing slightly. One contribution to the varying frequency was loose screws, which held the wing trailing edge to the rear spar. Once tightened, the repeatability of dynamic responses improved; however, it was during this phase of the testing that the FSM was destroyed due to transonic flutter at Mach 0.98. The only other flutter condition occurred at Mach 0.945. Throughout the flutter testing, a "chimney" of high dynamic response covering a wide range of dynamic pressures between Mach 0.98 and 1.00 was observed.

Reference

2. Schuster, D. M.; Spain, C. V.; Turnock, D. L.; Rausch, R. D.; Hamouda, M-N.; Volger, W. A.; Stockwell, A. E.; "Development, Analysis and Testing of the High Speed Research Flexible Semispan Model"; Aeroelasticity Section Report LMES ASR 97-01; February, 1997.

FSM MODEL DETAILS

Layout and Instrumentation

O PRESSURE TRANSDUCERS
- 10%, 30%, 60% and 95%
- 20% chord at 20%, 45% and 75%
- upper and lower surface

□ ACCELEROMETERS

Removable LE

Removable Tip Cap

Removable TE

Rigid-mounted Engines

Sealed gaps

Flaps

Rigid Fuselage Fairing

Tunnel Wall

Balance

Pedestal

Flexible Mounting Beam

120 Fuselage ESP Pressure Ports (7 chordwise locations)
Fuselage Length = 18.39 ft.
Wing Span = 4.86 ft.

Tunnel Turntable

Figure 2 Details of the Flexible Semispan Model (FSM).

3.2 Interim Test Program Evaluation

In the planning process for PCD2, the aeroelasticity ITD team identified the need for a new semispan wind-tunnel model for the purpose of measuring flutter at high angles of attack and with large control surface deflections. However, it has not been feasible in the past to scale and build models to meet stiffness and mass distributions required for obtaining flutter in the tunnel and strength necessary to sustain loads at high angle of attack or large control deflections. Ideally such conditions would be representative of actual flight conditions that an advanced HSR vehicle would have to endure in flight. A new model was envisioned which would be based on the Technology Concept Airplane. The model was therefore identified as the TCA1-FSM. However, changing funding scenarios in the HSR aeroelasticity area lead to an ITD decision that this new model concept was not within the resource capabilities of the WBS 4.2.6. Therefore, the model was removed from the formal plans of PCD2. The **TCA1-FSM requirement evaluation** milestone documents the ITD recommendation to delete the TCA1-FSM.

3.2.1 TCA1-FSM requirement evaluation

This milestone was completed by the Aeroelasticity ITD team through text that was published in the August 1997 Monthly Progress Report. The recommendation was that a separate model for high angle of attack studies not be built, but that the existing and planned models (RSM/PAPA, RSM/OTT/ and ASM) be used wherever possible to gather high angle of attack data.

3.3 Baseline II Wind Tunnel Models Database

Two additional test configurations were identified for the RSM in order to extend the usefulness of the model from a rigid testbed to a one-degree-of-freedom and then a two-degree-of-freedom testbed at a very minimal cost to the HSR program. As such, additional wind-tunnel testing was planned which would improve validation efforts for the various aeroelastic methods being evaluated. The planned RSM PAPA test was performed August 24 to September 16, 1998. The planned RSM OTT test, however, was not conducted prior to the September 1999 conclusion of this task.

3.3.1 RSM pitch-and-plunge apparatus (PAPA) test

The Rigid Semispan Model (RSM) was mounted to the Pitch And Plunge Apparatus (PAPA) in order to provide steady and unsteady wind-tunnel test data including flutter data for an essentially two-degree-of-freedom dynamic system. An initial test was performed in the Langley Transonic Dynamics Tunnel (TDT) in June 1995 as Test #508, which failed to generate the desired levels of dynamic response and did not encounter a flutter instability. Although this test installation included a shortened fuselage fairing as a result of PAPA geometry restrictions, it nevertheless did provide useful steady data pertaining to sensitivity to the east wall slot configuration. Results of this test led to the decision to conduct the RSM balance Test #520 with the TDT east wall slots closed.

Subsequent redesign of the shortened fuselage fairing and modification of the mounting system and ballast led to a successful test completed in September 1998 as TDT Test #530. Figure 3 shows the RSM with the redesigned fuselage fairing mounted in the TDT (the PAPA mechanism is out of sight behind the wall). This test produced unsteady model pressure, response, and stability measurements suitable for use in analysis/test correlation work.

Flutter testing of the RSM/PAPA model produced some interesting results. The measured Mach-Q flutter boundaries of the RSM/PAPA showed a dependence of the flutter boundary on mean angle of attack, and the absence of flutter at positive angles. The effect of mean angle of attack on the flutter boundary was observed across the Mach number range tested.

Support to the RSM/PAPA test was provided by Boeing and is documented in Reference 3. Pretest analysis centered on flutter prediction to determine the appropriate test configuration and test conditions to acquire useful data. The NASTRAN finite element model of the PAPA provided by NASA was refined and used to perform flutter sensitivity analyses based on doublet-lattice linear unsteady aerodynamics over a Mach range of 0.65 to 0.80. Investigations covered sensitivity of flutter to the amount of ballast weight added to the aft fuselage, to the test medium (air or R134a), to the inclusion of fuselage aerodynamics, and to the pitch and plunge DOF natural frequencies. An important conclusion of the study was that at least 20 lb of ballast would be needed to induce a flutter response.

During the wind-tunnel test of the RSM/PAPA, Mike Salzbrun (Boeing-Seattle) visited the TDT and brought with him the equipment for flourescent microtuft testing. Microtufts were applied to the upper wing surface of the RSM; this required a greater level of labor than anticipated. Difficulty with flash bulbs at total pressures below 500 psf, inability to provide phasing of the flash lights as a function of the frequency of the flap oscillations, and other inconveniences caused the resulting acquired data to be less comprehensive than desired.

References

3. NAS1-20220, Annual Report for Calendar Year 1998, Work Performed Under Airframe Materials & Structures - 4.2, Aeroelasticity - 4.2.6.
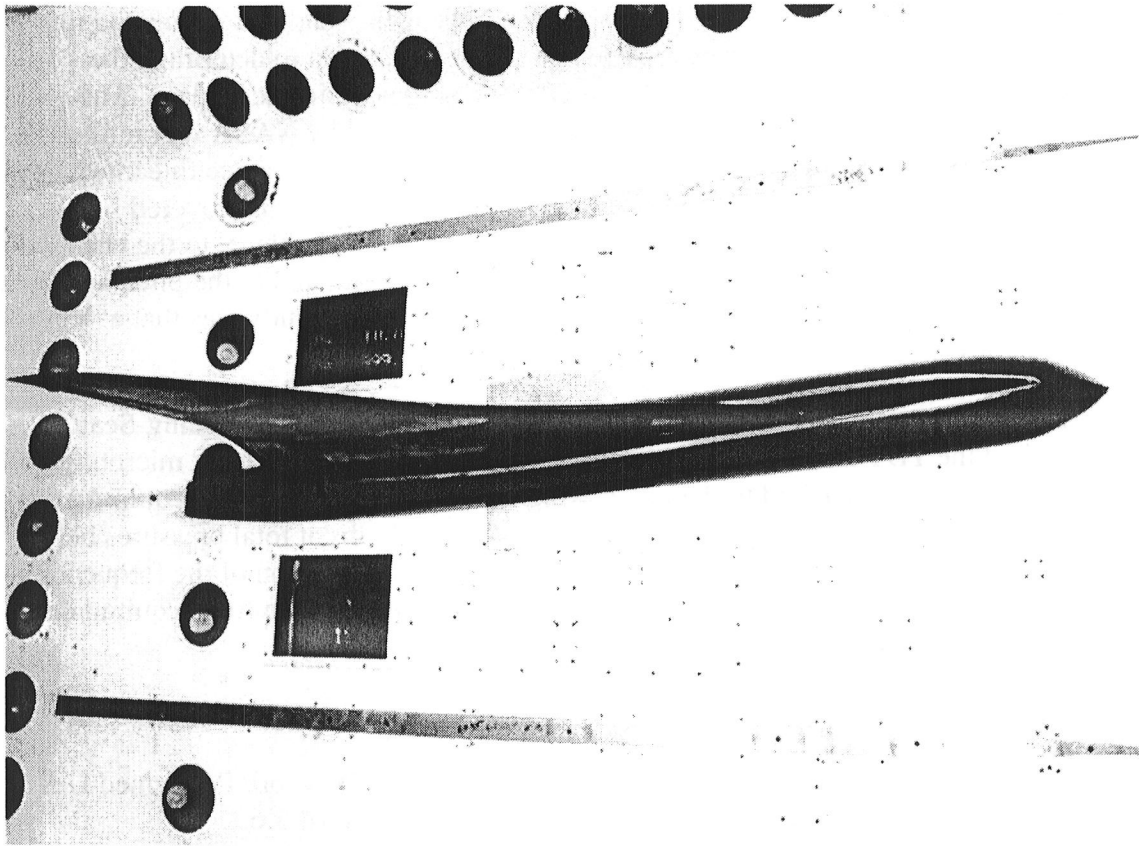
Figure 3 RSM/PAPA installed in the TDT for Test #530.

3.3.2 RSM oscillating turntable (OTT) test

The Rigid Semispan Model (RSM) was to be mounted to the Oscillating Turn Table (OTT) and tested in the TDT. The objective was to obtain steady and unsteady wind-tunnel test data, consisting primarily of model pressure measurements. Delays in completion of the OTT apparatus prohibited fulfillment of this milestone. In spite of the lack of experimental data, a certain amount of pretest analysis was performed using CFL3D Euler and Euler/Navier-Stokes unsteady aerodynamics. This support work is presented in Section 4.

3.4 ASE Wind Tunnel Models Database

In order to evaluate the aeroservoelastic characteristic and aeroelastic behavior of the Technology Concept Airplane (TCA), a full-span, aeroservoelastic, wind-tunnel model was planned to be designed and built for testing in the Langley Transonic Dynamics Tunnel (TDT). In order to improve the quality of data and reduce risk to this program three wind-tunnel models were planned as part of this effort. These are

the Aeroservoelastic Semispan Model (ASM), the Rigid Fullspan Model (RFM), and the Aeroservoelastic Fullspan Model (AFM). These models are referred to collectively as the ASE models. The ASM is a semispan model which utilizes the TCA wing.

Because of the September 1999 termination of the HSR program, the ASM was the only one of the ASE models to be designed and constructed. Cancellation of the RFM and AFM placed additional emphasis on the ASM to investigate aeroservoelastic characteristics and the interaction of fuselage flexibility in flutter. The ASM was designed to provide improved understanding of flutter mechanisms of the Technology Concept Airplane and, through parametric variations, provide flutter sensitivity information. In addition, the ASM was to be used, where possible, to investigate high angle-of-attack aerodynamics and flutter. Finally, the ASM was be used to provide a large database of frequency response functions relating control surface excitation to model response, as well as, serve as a testbed for investigating various control laws. Actual testing of the ASM was not performed before September 1999, forcing deletion of the ASM analysis/test correlation subtask.

3.4.1 Preliminary FFM specification

This work was to formulate specifications for and assist in the preliminary design of the ASE wind tunnel models including the Aeroservoelastic Semispan Model (ASM), the Rigid Fullspan Model (RFM), and the Aeroservoelastic Fullspan Model (AFM). A Model Oversight Team was formed in January 1997, which worked to develop a Specification Document for the ASE models which would define the models and provide a guide for potential vendors to follow in the design and fabrication of the models.

During August 1997, NASA requested that Boeing generate a Rough Order of Magnitude (ROM) estimate for the ASE wind tunnel models, at that time to include the ASM, RFM, and AFM. Model design and fabrication by Boeing Model Design was seen by NASA as a desirable alternate option to the use of third-party vendors. The resulting ROM estimate of $7.53 million for all three models (without spares) greatly exceeded the available $3.25 million budget. This was a factor in NASA's ultimate decision to concentrate the design and fabrication of the ASE models at NASA LaRC.

3.4.2 TCA parametric flutter analysis

This level 4 milestone was included in order to provide flutter sensitivity data with which to support scaling and design of the ASE wind tunnel models. These studies were based on airplane-scale finite element models of the TCA configuration which had been developed previously as part of the HSR DITS structural sizing effort. A

TCA Recommended Configuration was ultimately developed, which could preserve the desired soft, low frequency flutter mechanism in the tunnel environment while avoiding undesired explosive high frequency flutter. This Recommended Configuration then served as a target for further model scale analyses and design work.

Reference 4 provides the results of a study conducted at Boeing Seattle to investigate the flutter behavior of a planned TCA semispan model. Flutter sensitivity analysis was performed on both strength sized and strength+flutter sized versions of the TCA Elfini finite element model that was produced under the DITS work. Symmetric free and cantilevered boundary conditions were compared, as were the effects of nacelle and empennage aerodynamics. Results indicated that the type of flutter mechanism (low frequency, soft onset, inclusion of outboard engine pitching motion) that is desired in the ASE wind tunnel models test program can be expected to occur for the semispan model as well as for the planned full span flexible model. Also the sensitivity to the modeling of nacelle aerodynamics indicates that this would be a useful parameter in the test program.

Boeing Long Beach also performed a series of parametric analyses. The objective of this effort was to determine a configuration that could serve as a suitable configuration for designing and building the series of wind tunnel models. The approach taken to identify the design configuration was to start with the DITS TCA design, and investigate the flutter behavior of this baseline airplane in detail. This included analyses of all mass conditions at Mach numbers between 0.6 and 1.2. Most of this effort was performed under the DITS subtask, but some additional conditions were analyzed in order to cover the full mach range of the TDT. Once the flutter behavior of the baseline TCA was understood, a series of variations to the TCA were constructed and analyzed. For each variation, all mass conditions were again analyzed in a a mach range between 0.4 and 1.2 so that no relevant information would be missed. This required a total of 200 flutter analyses for each parametric variation (20 mass conditions, 5 Mach numbers, and two symmetry conditions) for a total of approximately 6,000 flutter analyses. Once the flutter analyses had been performed, the V-G and V-F plots were printed, and the impact of each variation on the FFM design (with secondary attention to the TCA vehicle) was assessed, and a candidate design configuration was identified. The recommended configuration was adopted by the NASA DBT, and the ASM was designed based on this configuration. This effort is documented in Reference 5.

References

4. Technical Milestone Report, "Flutter Sensitivity Study of the HSCT TCA Configuration as a Semispan Aeroelastic Wind Tunnel Model", DTF 26-1-07 dated November 5, 1997.

5. Parametric Flutter Analyses of the TCA Configuration and Recommendation for FFM Design and Scaling", December 12, 1997.

3.4.3 ASM model design support

Support by Boeing for the design effort for the ASE models, much of which is described in detail in Reference 3, was provided as follows:

Wind Tunnel Model Design Support

During November 1998, two engineers from Boeing Model Design traveled to NASA LaRC to review the ASM design effort, discuss design/fabrication issues, and identify areas of future Boeing participation. Much of their three-day trip was spent reviewing the model design and discussing fabrication issues.

A pressure tap layout for the ASM wing was generated and provided to NASA for their review. The suggested layout took into consideration knowledge and experience from previous HSCT aero models as well as paying special to details for measuring unsteady pressures due to flutter or forced harmonic oscillations of control surfaces such as the RCV.

ASE Models Actuator Design and Test Support

In February 1998, Boeing Flight Controls provided a document entitled "HSR Flexible Wind-Tunnel Model Actuator Test Plan Inputs". The document suggests objectives and procedures for the test plan of ASE wind-tunnel model actuators.

A memo entitled "Actuator Testing & Backup Structural Stiffness Effects (For ASE Model Testing)" was drafted and submitted to NASA for review in November 1998. The memo recommends several test conditions for determining the dynamic characteristics of the actuator, the control surface, and their dynamic interaction.

Preliminary Design Review for ASM Wind Tunnel Model

Boeing personnel participated in the Preliminary Design review (PDR) for the Aeroelastic Semispan Model (ASM) that was held at NASA Langley on August 18-20, 1998. In October, a report documenting Boeing's response to the ASM Preliminary Design Review was submitted to the ASE Models Program Management, the Aeroelasticity ITD Team, and the Structures and Materials TMT. The report was a critical review of the ASM preliminary design. The report recommended actions to address concerns that several important aspects of the model design were not adequately addressed or resolved.

References

3. NAS1-20220, Annual Report for Calendar Year 1998, Work Performed Under
   Airframe Materials & Structures - 4.2, Aeroelasticity - 4.2.6.

3.4.4 Materials characterization for the ASM

Materials Testing Support for the ASM Wind Tunnel Model Design Effort

Personnel and resources of Boeing Material Technology (BMT) were involved with
the ASE models support activities, performing a series of laboratory tests from
August 1998 into March 1999 at the request of the NASA ASM design/build team.
Graphite/epoxy as well as fiberglass/epoxy laminates that were fabricated at LaRC
for the ASE model effort were tested in the BMT labs both for mechanical properties
and for integrity of fabrication, with the level of porosity as one concern. BMT also
provided consultation in fabrication and testing technology to the ASM design team,
which included a trip by BMT personnel to Hampton in August for direct
consultation and familiarization with the NASA model shop composite process
methods.

Laminates were fabricated from 0.0005"(nominal thickness) graphite/epoxy prepreg.
Thickness measurements of the fabricated, flat panel, laminates consistently
measured ~50% thicker than anticipated. To investigate the excess thickness, BMT
performed photomicrographs and acid digestion on sample specimens. The
photomicrograph of laminate cross-sections was to determine ply quantity and
orientation. Acid digestion was to determine void content and fiber and resin volume.
Levels of porosity that were measured led to recommendations to the NASA team for
process improvements.

A subsequent batch of graphite/epoxy laminate samples were sent by NASA to the
BMT labs for mechanical property testing as well as for more photomicrograph and
acid digestion studies. After the decision early in 1999 to switch to fiberglass/epoxy
as the ASM material, mechanical property testing was performed as well on
fiberglass/epoxy samples provided by NASA.

The Coatings/Adhesives lab at Boeing Material Technology performed surface prep
on aluminum wing fixtures that were received from NASA. After phos anodizing and
priming of the surfaces to be bonded, they were returned to NASA.

A representative from Boeing Model Design spent the majority of the month of
September at NASA LaRC participating in the ASM design effort. While at LaRC,
he developed and refined NDE test plans for inspection of composite components of
the ASE wind tunnel models. Three stages of inspection were identified, each
corresponding to a stage of fabrication:

1) Wing Skin Laminate (porosity in graphite/epoxy laminates)

2) Skin-to-Core Bond (bond strength, delaminations)

3) Core-to-Core Bond (splice of upper and lower wing skin/core assemblies)

A Laminate Fabrication Test Plan was developed to gain an understanding of as received material form (graphite-epoxy laminate), layup and bagging techniques, tooling and cure conditions. The Plan was submitted to NASA in October for review.

A memo entitled "Secondary Bonding of Wing Root Fixtures" was drafted and submitted to NASA for review. The memo provides information about preparing both metals and laminates for secondary bonding operations.

3.4.5 ASM related airplane scale analysis

Delivery of Airplane-Scale Recommended Configuration FEM

After the recommended configuration was defined as a variation of the TCA configuration, the finite element model (FEM) of the recommended configuration was delivered to NASA LaRC. This model served to define the target mass and stiffness properties that the ASE wind tunnel models should be designed to meet. As part of the model delivery, a Boeing engineer traveled to LaRC and spent one week training LaRC personnel in the contents of the finite element model and how it could be used in the model design process.

TCA Outboard Wing Flow Separation and Jig Shape Study

A serious concern in the ASE models was the aerodynamic behavior of the outboard wing and how the model jig shape could be defined to minimize the problems. In order to address these concerns, CFD analysis was performed in TLNS3D-MB and in CFL3D-AE.BA to determine the levels of flow separation on the outboard wing. Flow visualization was performed for solutions at Mach 0.95 and 1.2, and at angles of attack of 2.9, 3.25, 3.5, 3.75, and 4.4 degrees. It was determined that flow separation appeared on the outboard wing panel at relatively low angles of attack. For example, at Mach 0.95 and 2.9 degrees angle of attack, the separated region covers approximately the first 10% chord of the outboard wing. In addition, a jig shape analysis was conducted in which the aerodynamic loading on the wing was determined for various jig shape concepts. The jig shape was eventually determined to be the undeformed shape of the airplane, as this resulted in the most reasonable spanwise load distributions and less outboard wing separation than the other possibilities.

Flutter Sensitivity of TCA

A flutter sensitivity analysis of the strength-sized Elfini (airplane scale) FEM of the TCA was performed. The sensitivity analysis was performed to provide insight into a similar analysis being performed at Long Beach for the Recommended Configuration. The analysis focused on the airplane low-frequency flutter mode at Mach 0.95 for mass case MT-1 (MTOW). The analysis determined the sensitivity of the flutter dynamic pressure to the number of modes included in the flutter analysis and to the elimination of individual modes. The analysis indicated that approximately 20 modes should be included in the free-free symmetric flutter analysis of the TCA. Further, modes 17 and 18 appear to have a significant contribution to the low frequency flutter mechanism at Mach 0.95 and mass case MT-1.

Additional sensitivity studies were also performed. Investigations included the effect of control surface stiffness on overall wing stiffness and the impact of an overly stiff wing caused by a model-scale minimum skin gage that is too large to allow exact scaling.

TCA Configuration Data Provided to NASA

Lofts of the TCA wing, horizontal tail, vertical tail, and fuselage were provided to LaRC model designers in the form of IGES files. A wireframe of the TCA Structural layout was provided to LaRC model designers in the form of IGES files. A memo describing the hinge line definitions and control surface boundaries for the TCA was drafted and provided to NASA. Additionally, an IGES file containing this information was created and provided to the LaRC model designers. Centerline drawings of the TCA engines were provided to LaRC model designers in the form of IGES files.

Determination of internal structure shear stiffness requirement

The TCA main wing box was a multicellular box. The number of cells varied from inboard to outboard. This multicell box was going to be idealized with a full depth honeycomb in the construction of the ASM wing. A series of analyses were performed to determine if the idealization would produce the desired torsional as well as bending stiffness. All analyses were performed on the full scale FEM. The shear webs were removed from the model and solid elements were generated and inserted into the FEM. The shear modulus of the paper honeycomb was scaled up to airplane scale and assigned to the solid elements. The outboard wing was cantilevered at the inboard/outboard break and static loads were applied at the tip. Acceptable static correlation was achieved.

The mass of the shear webs that had been removed was determined and the density of the added solid elements was then adjusted to give the same weight. A cantilevered vibration analysis was performed and the results were compared with the TCA

baseline FEM. Acceptable dynamic correlation was achieved and the design approach was validated.

Determination of the outboard wing leading and trailing edge attachment

The TCA leading and trailing edges were comprised of a series of discrete control surfaces. Keeping this design feature would increase the complexity of the ASM and it was desired to idealize the design by having continuous leading and trailing edges. To determine if this idealization could be made, all the control surfaces were rigidly attached to each other and to the primary surfaces and the resulting vibration modes and flutter boundaries were determined. The results indicated that this idealization maintained the desired vibration and flutter behavior.

Determination of the engine pylon stiffness distribution

NASA requested that Boeing determine the stiffness distribution of the pylon in the TCA Recommended Configuration. The pylon section properties were determined, including vertical and lateral bending stiffness as well as torsional stiffness. A stiffness curve was then faired through the discrete sectional properties. An equivalent beam model was developed and static analyses were performed and correlated with the TCA FEM. The sectional mass properties were determined and connected to the beam model and cantilevered vibration analyses were determined. Finally, the resulting beam model replaced the TCA Recommended Configuration pylon and vibration and flutter boundaries were determined, verifying the stiffness and mass distribution idealizations, which were delivered to NASA.

Determination of the required number of outboard wing shear webs

The NASA design and build team had determined that the main box of both the inboard and outboard wings should have shear webs at the same locations as the leading and trailing edge spars on the TCA. Fabrication of a model with these webs would be more difficult than if no webs were present. Boeing performed flutter and vibration analyses with and without the shear webs and determined that the core provided enough shear stiffness and that no additional shear webs were required, simplifying both the design and fabrication process.

Determination of the outboard wing trailing edge flap 2 rotation frequency

NASA was concerned about the effect of a failed hydraulic actuator powering flap 2. Boeing performed analyses to determine the flutter characteristics of a variation of flap frequency from 0 to 20 Hz. It was shown that as the flap frequency dropped below about 5 Hz, a significant drop in flutter dynamic pressure was seen. As the flap frequency dropped to zero, the flutter dynamic pressure continued to drop to almost zero. This led to a design goal for the actuator/flap system that the flap rotation frequency should be as high as possible.

Determination of the modal participation in the flutter mechanism

It was desired to determine which of the TCA vibration modes were participating in the flutter mechanism. It was thought that determining which modes were contributing to the mechanism would influence the idealization/design process. Determination of modal participation was accomplished by deleting an individual mode and then determining the flutter boundary. This analysis revealed that flexible modes 1, 2, 3, 4, 5, 8 and mode 17 were "significant" contributors to the 17 Hz flutter mechanism. This was a surprising result as mode 17 was 83 Hz and involved a lot of outboard wing torsion. An additional study was performed which varied the frequency of the 83 Hz mode by +/-30%. The results of this analysis indicated that the frequency of this mode could be significantly changed and not significantly influence the 17 Hz flutter mechanism. This allowed the designers greater latitude in their design.

Determination of the 2 point mounting system

The ASM was envisioned as a cantilevered semi span model, but the S&C community desired that the semi-span model replicate the free-free symmetric behavior as closely as possible. Boeing performed a series of analyses on a variety of configurations to determine if any mounting scheme could replicate this behavior. The node points of the modes that were "heavily" participating in the flutter mechanism were determined, and an "average" node location was determined. The TCA was then restrained at these "average" node points in the vertical direction. This configuration produced a reasonable flutter envelope. The addition of vertical translational degree of freedom produced a significantly better match. (This vertical degree of freedom was assigned a stiffness of 50 lb./in.) consequently the NASA design and build team set about designing a two point mount system that could allow these two vertical translational degree's of freedom with acceptable low stiffness to get acceptable flutter and dynamic response.

Mass Panel Data for ASE Wind Tunnel Model

A request was made by the LaRC ASE wind-tunnel model design/build team to provide a mass panel breakdown of the finite element model of the recommended TCA configuration. The request specified that mass, c.g., and mass moment of inertia was to be determined for a provided panel layout of the TCA planform. To fulfill this request, some effort was required to modify a pre-existing process used with ELFINI finite element models. In a relatively short period of time the process was modified and the requested information was delivered in the form of ASCII files containing mass, c.g., and inertia for each mass panel. In addition to the requested information, the panel mass was divided into mass "types" - theoretical, fixed, added, double fuselage, fuel, and payload mass. This information was provided in the form of an Excel spreadsheet which plotted the nodal masses contributing to each mass panel

and also allowed filtering based on mass types, panel number, and airplane section number.

3.4.6 ASM model scale analysis

Translation of Recommended Configuration to Model Scale

The TCA FEM that was delivered to NASA was an airplane scale FEM. All design work was being performed in model scale and NASA desired a FEM of the TCA in model scale. Boeing then generated a Fortran program that scaled each card in the NASTRAN bulk data file down to model scale. Vibration and flutter analyses were performed on this model and the results were an exact mathematical scaling of the full scale TCA FEM. This model scale FEM was then used as the validation platform for evaluating idealizations of various components. The validation process in brief involved removing a TCA component and replacing it with the idealized component and performing analyses on the resulting "mostly TCA" and "a little model" structure to verify the design approach. If the results were acceptable, then the component was validated. If not, then the source of the discrepancy was known.

Development of Wing Ballast Masses

The inboard wing and strake both needed to be ballasted to achieve the design mass properties. Boeing developed a process that would generate the mass properties of both the TCA and the unballasted model on a discrete set of ballast points. The unballasted model mass was then subtracted from the TCA to produce the ballast weights. These weights were then input into the model analysis and vibration and flutter analyses were performed and compared with the design.

Determination of ideal ply lay-up schedule for ASM wing

The NASA design and build team selected a 0.00075" unidirectional Gr/Ep prepreg material to be used in the wing skins. Many difficulties were encountered with this material and the wing skin material was switched to fiberglass/epoxy around December 1998. NASA requested Boeing to design a new set of idealized (i.e. non itegerized) wing skins out of the unidirectional fiberglass prepreg material. Boeing then designed the new idealized wing skins. This idealization was validated statically and dynamically.

Validation of ASM Wing Properties

During the design process there were many changes to the wing design that required verification. Boeing developed a process to verify the effect wing design changes. This process included "stitching" the model wing onto the model scale TCA FEM. A division between the wing and fuselage was determined and the TCA wing was removed from the TCA FEM (all analyses in model scale). The model wing was then

imported into the airplane FEM and attached to the remaining TCA components. Vibration modes and flutter boundaries were determined for this configuration. This process provided an excellent platform from which components could be validated and verified.

Determination of the fuselage stiffness distribution

NASA requested that Boeing develop a stiffness distribution of the fuselage of the recommended configuration in order to design the fuselage spar. Boeing determined the discrete sectional properties at many section cuts along the fuselage and then faired a curve through these points to obtain stiffness curve. A beam model was constructed from this curve and static stiffness behavior was evaluated. The fuselage was then discretized and mass properties were determined. These mass properties were then included with the stiffness distribution and free-free vibration modes were generated and compared. In addition, Boeing performed a set of analyses that helped determine the size and location of the wing/fuselage attachment brackets that would not cause unacceptable local stiffening of the wing, and would still provide sufficient wing-to-fuselage attachment.

Validation of ASM Fuselage Properties

As stated in the *Validation of ASM Wing Properties* above, the same methodology was employed for the verification/validation of the fuselage design. Instead of the wing being removed from the fuselage, the fuselage was removed from the wing and replaced by the idealized beam fuselage. Again, as many TCA components as possible were kept in the analysis so that any deviations from the design could be attributed to the fuselage alone. Vibration and flutter analyses were performed to verify the designs.

Elfini Finite Element Model Version of the TCA Recommended Configuration

The Elfini FEM of the TCA (converged DITS strength optimization result) was modified by stiffening of the outboard wing, doubling the fuselage mass, rigidization of actuators, and addition of the ride control vane. The resulting flutter analysis scaled to the TDT operating environment showed the same flutter characteristics as the Config. 3 NASTRAN analysis. The model was for use in control law sensitivity investigations for the ASE wind tunnel models.

Finite Element Model of the ASM Wind Tunnel Model

Starting in June 1998 an effort to provide analytical support for the ASE models design team was initiated. Structural modeling of the ASM design in both Elfini (finite element) and ELAPS (equivalent plate) systems was started, in order to quickly as possible obtain dynamic response predictions before the design was finalized. The ELAPS effort continued into September, at which time the Elfini effort was selected as the priority for continued effort.

The Elfini FEM was built based upon the ASM design (circa Sept '98). Preliminary results from this model showed some discrepancy with results from a scaled TCA FEM, with the ASM model FEM overly stiff relative to a scaled airplane FEM.

Preliminary flutter analysis for the ASM wind tunnel model FEM was performed. Initial results indicated a flutter boundary above 200 psf and flutter frequencies above 23 Hz.

A summary report describing the status of and results from the Elfini finite element model of the ASM was issued in November 1998.

3.4.7 ASM model critical design review

The CDR was held April 28-30, 1999 at NASA Langley Research Center. The Review consisted of presentations by the NASA model design team and a presentation by Boeing describing scaling and FEM analysis of the model wing design. The primary objective of the Review was to demonstrate to a review committee that: (1) Model design is feasible and buildable, (2) Model will exhibit satisfactory dynamic and flutter characteristics, (3) Model will be completed on schedule, and (4) Sufficient fabrication funds remain to complete model. The CDR presentation overall met with strong support from the review committee, and the CDR was successful. Feedback from the committee included some general comments followed by issues falling under three headings: Technical, Schedule, and Resources.

4. Analysis/Test Correlation

4.1 Code Assessment I

Based on analysis/test correlation with data obtained through the **Baseline I semispan models wind-tunnel test database**, a preliminary code assessment was made with regard to analyses accuracy in predicting loads and flutter. The Code Assessment I contract deliverable requirement was fulfilled with Reference 6, an assessment of evaluated analysis techniques which indicates their relative accuracy. The summary below highlights its content.

The focus of this assessment is on several CFD codes which have been applied to provide aerodynamic loads for the aeroelastic analysis of HSCT configurations. These codes are (in order of increasing flow-physics-modeling fidelity): PANAIR, TRANAIR, and CFL3D. In addition to these codes, Linear Theory methods, specifically Doublet Lattice Methods (DLM), are occasionally used as a reference, but these methods did not undergo a rigorous analysis/test correlation for the HSR wind-tunnel models and therefore are not the focus of this assessment.

The following is a brief summary of each code and the theory contributing to their modeling of the flow.

The doublet lattice method is a linear lifting surface technique for steady/unsteady aerodynamics developed in the 1960's, and is an industry standard unsteady aerodynamics method. The doublet lattice method and its supersonic counterpart ZONA51 are implemented in MSC/NASTRAN, and a similar singularity method is available in ELFINI, and these codes as well as PANAIR were used in HSR/DITS sizing. Due to modeling restrictions in the lifting surface methods, they are primarily applicable to computing loads on thin wings and slender bodies. Similar to other linear potential codes such as PANAIR, these techniques do not capture transonic or viscous effects.

PANAIR and TRANAIR have been developed at and are widely used at Boeing. The two codes share a common geometry panel input and post-processing features. PANAIR is a higher-order panel method which solves the linearized potential-flow boundary-value problem. Complex three-dimensional configurations, such as the HSCT (wing/body/nacelle/diverters), are discretized using 3-D surface panels (networks). PANAIR is suitable for modeling subsonic and supersonic flows, where viscous effects are not prominent flow features. TRANAIR is a system of computer programs that solve the full potential flow equations with a coupled boundary layer. The configuration geometry and the flow field are discretized independently such that the surface of the configuration is divided into surface networks and the flow field is divided into a locally refined rectangular grid. The rectangular field grid is automatically generated, and then iteratively adapted in the solution process as the

flow field evolves. TRANAIR can be coupled to a boundary layer solution to account for some of the viscous effects. Thus TRANAIR is suitable for modeling subsonic, transonic, and supersonic flows; however, it cannot accurately predict flows dominated by viscous effects (other than boundary layer), nor can it accurately predict flows dominated by *strong* (non-isentropic) transonic flow effects. TRANAIR is a mature code for subsonic applications in its range of applicability, and recently has seen significant usage in the HSCT applications particularly in the supersonic range.

CFL3D is a Reynolds-Averaged thin-layer Navier-Stokes flow solver for structured multi-block grids developed at NASA Langley Research Center, and is the paramount code being assessed. The flow field is discretized using blocks of body-fitted structured grids which can be patched and/or overlapped to fill the computational domain. CFL3D is applicable across the Mach range of interest and is particularly well suited for modeling viscous dominated flows with leading-edge flow separations. For unsteady flow computations, CFL3D features a two-tier time integration scheme. This scheme uses subiterations at every time step to eliminate linearization errors which degrade numerical accuracy and stability. Under the HSR Aeroelasticity task, the CFL3D solver has been extended into a nonlinear aeroelastic analysis tool. This tool consists of three main elements: the baseline CFL3D solver, an efficient and accurate structural integration package patterned after that found in the CAPTSD code, and a newly developed fast grid perturbation module (=FlexMesh). Of these three CFD codes, CFL3D is best suited to model the physics of the nonlinear flow phenomena that may impact flutter.

There is a price to pay for solution fidelity/accuracy in the form of extended modeling time (grid generation), slow turn-around (supercomputing resources - in-core memory, CPU time), and the support resources required to monitor and evaluate solutions. These costs are too expensive to blindly apply a higher fidelity code for all flow conditions. In general, codes with simpler flow physics are usually simpler and cheaper to run. As an aside, correction procedures for updating Linear Theory based on wind-tunnel data or high-fidelity CFD results may be a simpler approach. These procedures may reduce costs while maintaining fidelity. That being stated, this interim assessment makes no attempt to weigh differences between the codes in terms of cost/simplicity vs. fidelity/accuracy. Our current assessment attempts to focus only on solution accuracy relative to wind-tunnel test data.

The steady-flow analysis/test correlation results for the RSM (clean-wing configuration) are summarized for several Mach number ranges in Table 1. This summary is based on a limited correlation at 0 and 2 degrees angle of attack.

Table 1 Steady-flow correlation assessment for the RSM (clean-wing configuration); Mach range for 0.70 to 1.15; angle of attack limited to 0 and 2 degrees.

Codes	Mach Number Range		
	0.7 to 0.9	0.9 to 1.05	1.05 to 1.15
Linear Theory	✔+	✔-	✔-
PANAIR (A502)	✔+	✔-	✔-
TRANAIR (w/ Boundary Layer)	✔+	✔	✔+
CFL3D (Navier-Stokes)	✔+	✔+	✔+

✔+ Good; ✔ Adequate; ✔- Poor

CFL3D demonstrated good overall correlation for the limited angles of attack correlated, provided that viscous effects are modeled in the transonic flow range. TRANAIR with a coupled boundary layer solution provided satisfactory overall correlation for the limited angles of attack. Both PANAIR and Linear Theory demonstrated good correlation for the subsonic conditions, but showed poor correlation in the transonic and low supersonic range.

The unsteady-flow correlation for the RSM was limited to wing pressure data for flap oscillations at Mach 0.80 and 2 degrees angle of attack. Overall, the analytical codes - PANAIR, TRANAIR, and CFL3D - predicted the magnitude of the unsteady pressure to be higher than the measured data.

The FSM correlation is clouded by the uncertainties in the wind tunnel model definition and test data. In spite of these deficiencies, there was good correlation with wing force and moment data, and pressure data, at subsonic and supersonic conditions, but the correlation was not completely satisfactory because of discrepancies with measured wing twist and defection data. Flutter analysis produced encouraging correlation with the limited flutter and dynamic response data for the FSM, in spite of uncertainties in the test configuration. The flutter test data was obtained at low angles of attack to reduce the wing loads.

The **baseline I semispan models wind-tunnel test database** has provided a set of force and pressure measurements that contributes to the multi-step code validation process, but falls short of the original goals for the database and has limited value for direct aeroelastic code validation. Many of its shortcomings were to have been rectified by the **Baseline II wind tunnel models database** and the **ASE wind tunnel models database.** Unfortunately, only the RSM Pitch and Plunge Apparatus (PAPA) component of these latter databases was completed before contract termination in September 1999. Results of other important test plan elements, the RSM Oscillating Turn Table (OTT) test and the series of ASE models tests, were not available. The OTT test was to have provided additional unsteady pressure data for the RSM, but for

a wider range of flow conditions. The ASE models tests would have provided static and dynamic aeroelastic data for a TCA configuration with canard.

Recommendations listed in Reference 6 emphasize the need for improving the fidelity of test model definition and calibration, and more comprehensive pre-test analytical predictions. There is also a need to define/understand tunnel correction factors and uncertainty levels of the data.

Reference

6. Technical Milestone Report, "Code Assessment I Based on Baseline I Semispan Models Analysis/Test Correlation," dated March, 1998.

4.1.1 RSM analysis/test correlation

In support of the Code Assessment I milestone, this subtask includes correlation of analyses with test results obtained from NASA testing of the rigid semi-span wind tunnel model representing the Reference H planform (RSM) mounted on the balance. References 7 and 8 are the associated contract deliverable reports, Reference 9 contains additional results for CFL3D static and dynamic flap analysis/test correlation, and Reference 10 has additional results for TRANAIR analysis/test correlation with boundary layer effects.

The RSM wind-tunnel test data used to formulate this interim code assessment was obtained during TDT Test 520 conducted during March and April 1996. Data from an October 1994 test of the RSM (Reference 11) was not used because it was determined that the data was biased by wind-tunnel side-wall slot effects. The RSM test(s) provided balance and surface pressure (wing/body-fairing) data for static flow conditions covering a Mach number range from 0.7 to 1.15 and an angle-of-attack range between -2 and 8 degrees. Additionally, dynamic surface pressure data was obtained for a harmonic trailing edge flaperon oscillation at several frequencies.

Steady-Flow Correlation

An enlightening summary of the RSM steady-flow correlation is illustrated in Figure 4; which shows a comparison of wing lift-curve slope over the Mach number range from 0.70 to 1.15 for the RSM clean-wing configuration. The correlation is good/fair for all the codes up to Mach 0.90. There appears to be an offset between measured and computed lift curve slopes. Generally, at at Mach 0.95 the overall correlation rapidly declines. The shape of the Euler-computed lift-slope curve follows the experiment quite well if the shift at Mach=0.95 is ignored. This shift comes about because the Euler solutions lack the decambering effect of the boundary-layer flow. Thus, the Euler solutions overpredict the wing shock strength and put the shock to far aft. This issue vanishes for subcrtical flow and for supersonic freestream where the

shocks are anchored at the wing trailing edge. The scatter in the results, near the transonic range, draws attention to the aerodynamic predictions in this Mach range, and hence illuminates the crux for the analysis/test correlation studies. It should be noted that even though the lift-curve slope from Linear Theory and PANAIR at Mach 0.95 correlates well with the data, this good correlation is an anomaly. Details of the sectional load (based on measure sectional pressures) show large discrepancies.

The effects of viscosity were investigated with TRANAIR and CFL3D. Figure 4 illustrates an expected conclusion - viscous boundary layer effects are important for accurate load prediction especially in the transonic flow range. This is observed by comparing the TRANAIR inviscid and BL results, or the CFL3D Euler and N-S/SA, at Mach 0.95. Both sets of results show improved correlation with the data when viscous boundary layer effects are modeled in the flow analysis. A closer look at the lift-curve slope for TRANAIR (BL) and CFL3D (N-S/SA) is shown in Figure 5. In general, at the moderate angles of attack of the test-database flow conditions, the modeling of the viscous BL does not appear as important in the subsonic and supersonic regimes.

The dominant flow feature at Mach 0.95 having the largest impact on the computed results is a transonic shock situated on the wing. The ability of the codes to accurately predict the strength and location of this shock has a significant effect on the steady air-loads. Figure 6 shows the predicted shock location in a series of plots which present wing surface pressure coefficient at four wing semi-span locations. Calculated results are shown only for TRANAIR with boundary layer and CFL3D Navier-Stokes solutions; since these are the most applicable solutions for these conditions. As shown in the series of plots, the shock varies in strength and location along the wing span. Near the wing root the shock is located near the 88% local chord and near the wing tip the shock has diminished. Inviscid results at these conditions over-predict the shock strength for a given angle of attack and contribute to inaccurate wing load distributions and total wing integrated loads.

Based upon the RSM steady-flow analysis/test correlation, the following assessment is made. PANAIR predicts loads that are satisfactory in the subsonic flow range, but in the transonic and low supersonic range (0.9 to 1.15) the predicted loads do not accurately represents the wind-tunnel loads. TRANAIR is regarded as being sufficient for predicting loads across a Mach range from 0.70 to 1.15 provided that 1) the angle of attack is moderate to low ($| \alpha | \leq \sim 3$ degrees, high leading-edge suction peaks may cause numerical trouble) and that 2) viscous boundary layer effects are modeled in the transonic flow range. Similarly, CFL3D demonstrated good overall correlation, for the limited angles of attack of the correlation, provided that viscous effects are modeled in the transonic flow range.

Unsteady-Flow Correlation

The unsteady-flow correlation was far less extensive than the steady-flow correlation and firm conclusions for the code assessment cannot be reached. The amount of test data was limited to a few harmonic flap oscillation cases at Mach 0.80 and 2 degrees angle of attack. At these flow conditions, wing unsteady surface pressures were compared for a flap-deflection amplitude of ±2 degrees at frequencies of 1, 2, and 5 Hz. Overall, the codes predicted the unsteady pressure magnitude higher than the measured data as shown in Figure 7. In general, both PANAIR and TRANAIR demonstrated good code-to-code correlation. Both codes use a linear harmonic perturbation analysis about the steady-state solution. The addition of a static boundary layer model in the TRANAIR analysis had little impact on the predicted unsteady pressures as expected for this flow condition. CFL3D Euler and Navier-Stokes results demonstrated a similar trend of predicting the unsteady pressure magnitude higher than the measured data; although for time-marching calculations the results drew attention to temporal convergence concerns. Because of these concerns, the effect of viscosity could not be reliably assessed. An alternative approach utilizing CFL3D's dynamic pulse technique produced results that demonstrated encouraging correlation with test data. These N-S results also predicted the magnitude of the unsteady pressures to be higher than the data and may have suffered from similar temporal convergence concerns. In summary, all the codes and techniques predicted the magnitude of the unsteady pressures to be higher than the measured data and no code was clearly more accurate than the other two. In addition, the measured unsteady data are limited and subject to the uncertainty of the RSM data.

References

7. Technical Milestone Report, "Rigid Semispan Model (RSM) Analysis-Test Correlation," CRAD-9408-TR-2433 dated October 25, 1996.

8. Technical Milestone Report, "Correlation of A502 (PANAIR) and TRANAIR Inviscid Results with NASA Langley TDT Test 520 Data for the HSR Rigid Semi-Span Model," DTF 26-2-01 dated March 4, 1997.

9. Technical Milestone Report, "Rigid Semispan Model (RSM) with Flap Analysis-Test Correlation," CRAD-9408-TR-3691 dated September 15, 1997.

10. NAS1-20220, Annual Report for Calendar Year 1997, Work Performed Under Airframe Materials & Structures - 4.2, Aeroelasticity - 4.2.6.

11. NAS1-20220, Airframe Integration Task 17 (Aeroelasticity and Structural Dynamics Subtask 1) Final Report, dated March 31, 1996.
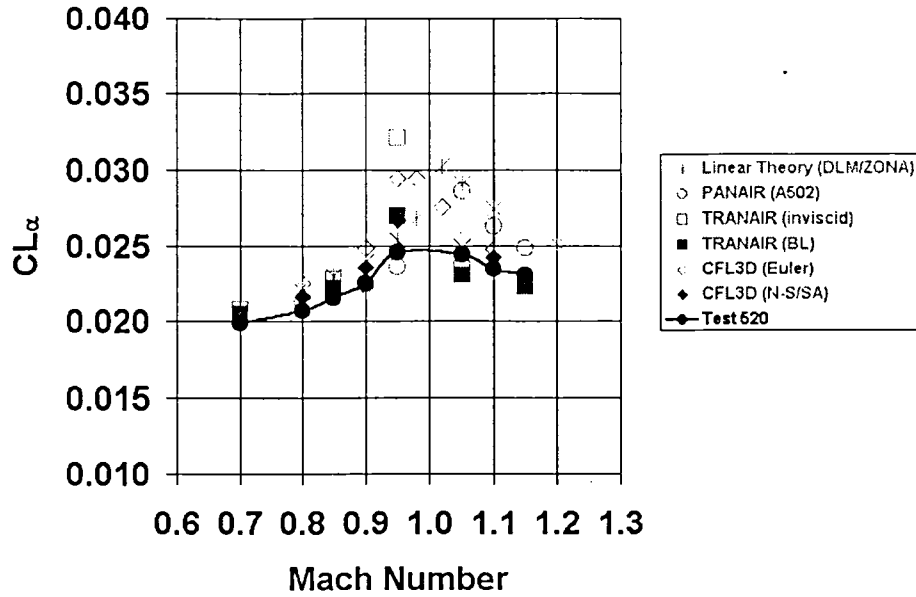
Figure 4 Variation of computed and measured lift-curve slope with Mach number for the RSM (clean wing).
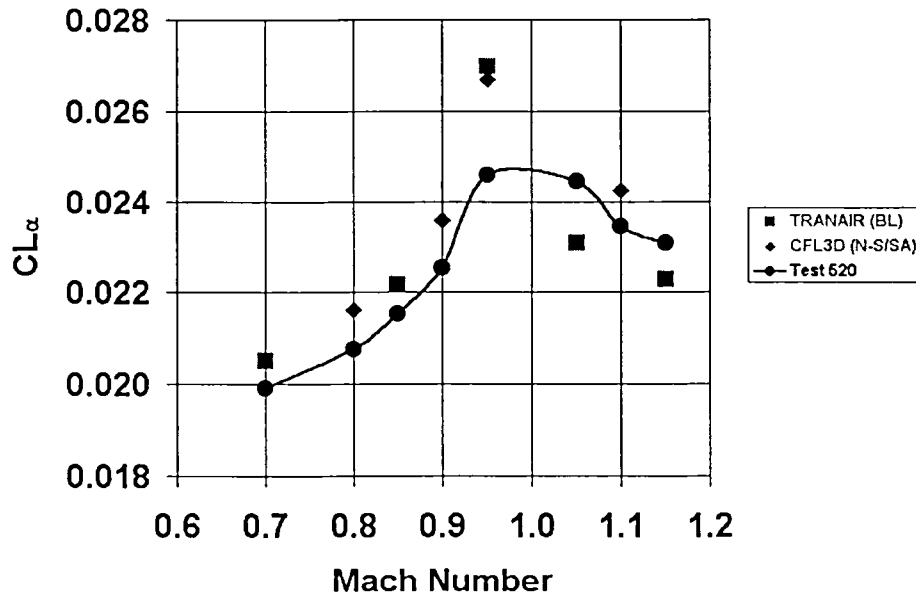

Figure 5 Variation of computed and measured lift-curve slope with Mach number for the RSM (clean wing); selected "best" codes/correlation.

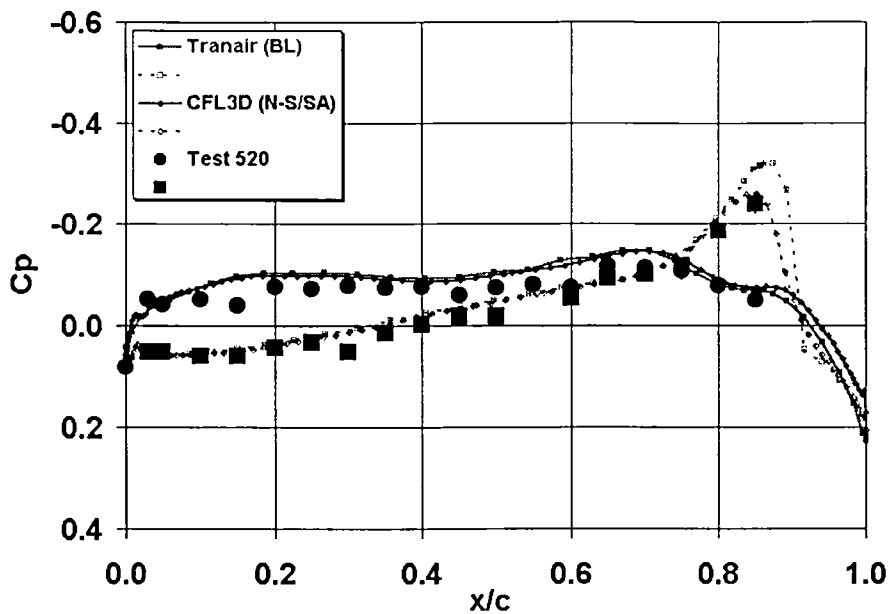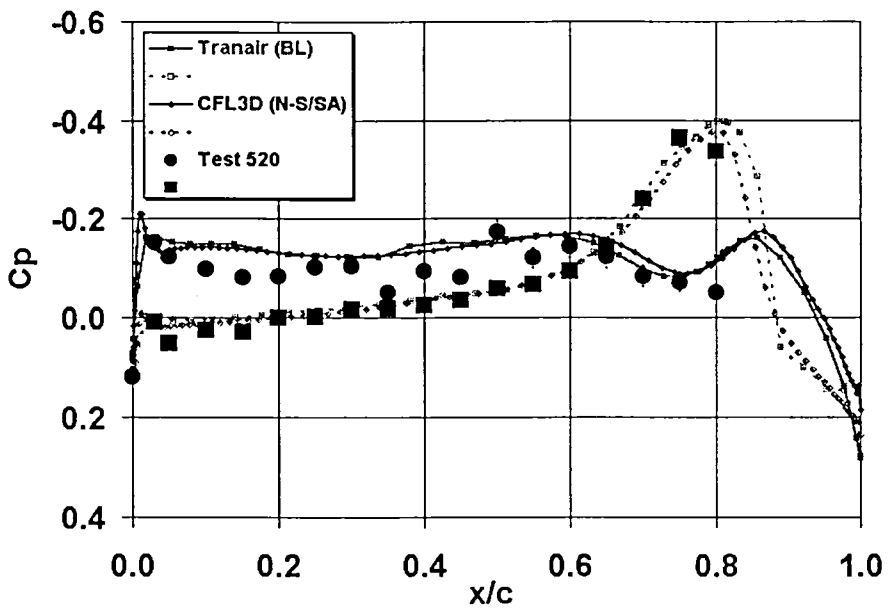Figure 6 Wing surface pressure coefficient for the RSM at Mach 0.95, alpha=2 degrees; (eta=0.10).
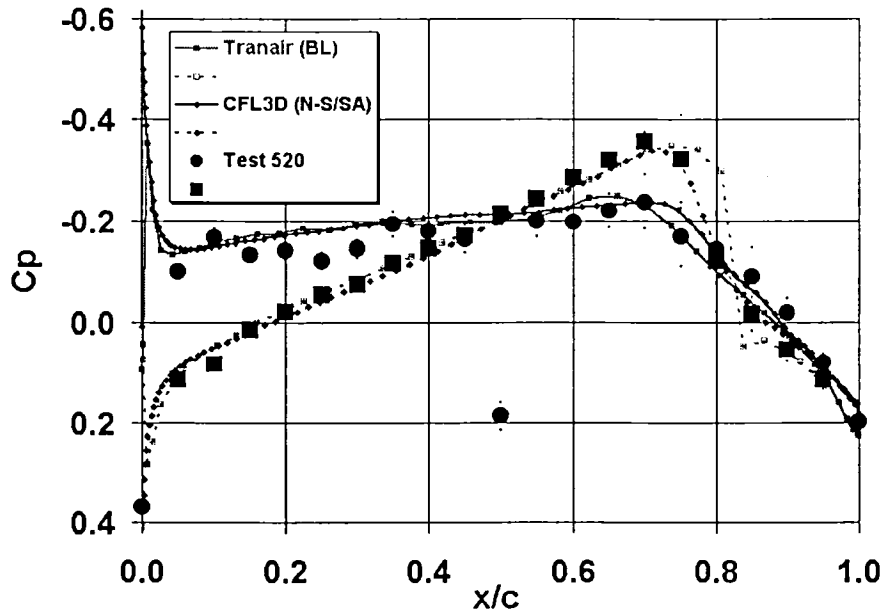

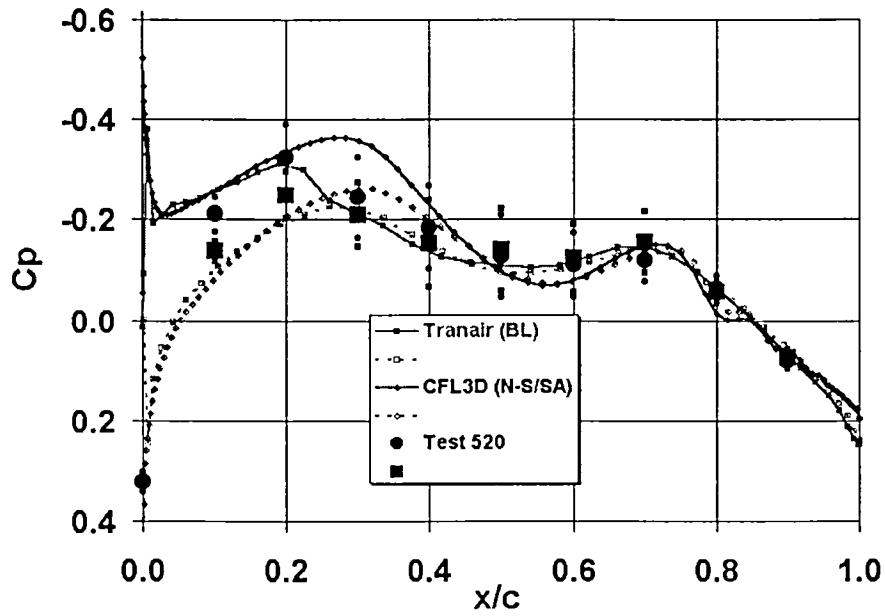Figure 6 (continued); eta=0.30.
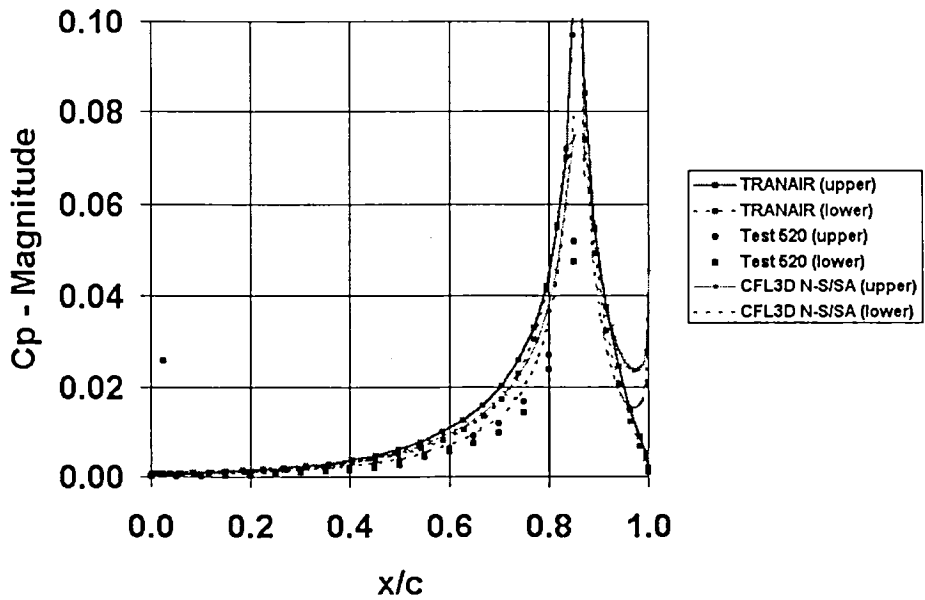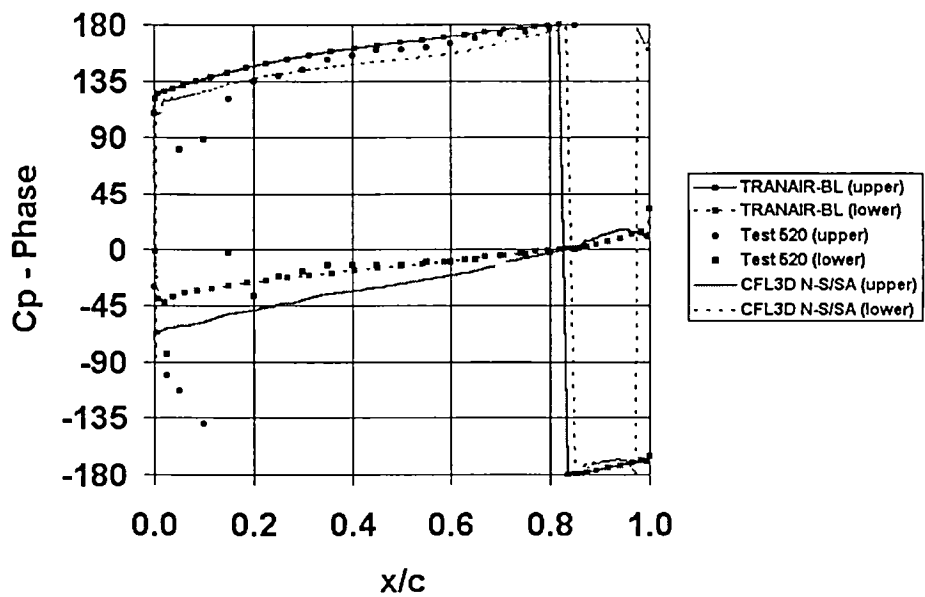
Figure 6 (continued); eta=0.60

Figure 6 (continued); eta=0.95

(a) Magnitude

(b) Phase

Figure 7 Unsteady wing surface pressure at h=0.10 for a harmonic flap oscillation of the RSM at Mach 0.80; α = 2 degrees; δ_0 = 0 degrees; δ_1 = 2 degrees; and f = 2 Hz.

4.1.2 FSM analysis/test correlation

In support of the Code Assessment I milestone, this subtask includes correlation of analyses with test results obtained from NASA testing of the flexible semi-span wind tunnel flutter model representing the Reference H planform (FSM). References 12 and 13 are the associated contract deliverable reports.

The FSM test provided, as did the RSM, balance and surface pressure data for static flow conditions, though for a flexible aeroelastic model. Dynamic aeroelastic data was obtained during a flutter-testing phase. It was during this testing phase that the FSM was destroyed due to transonic flutter at Mach 0.98. The only other flutter condition for the FSM occurred at Mach 0.945. In addition to the two "hard" transonic flutter points, there were several instances of high dynamic response (sometimes characterized as "soft" flutter) in a narrow chimney between Mach 0.98 and 1.00. This is a very challenging data set for analysis/test correlation because the "hard" flutter boundary only contains two points, and the chimney of high dynamic response is highly Mach dependent and probably very nonlinear in nature.

Several additional, purely structural-dynamic, complications make the aeroelastic code assessment difficult. One complication is the variation in dynamic behavior exhibited by the FSM as the test was in progress, leaving in question the applicability of the correlated finite element models at the test points. A second complication is that a comprehensive GVT was not performed on the FSM for the in-tunnel flutter test configuration, which made the GVT correlation effort a less reliable multi-step process.

Analytical Models

As part of the FSM correlation study, two finite element models (FEMs) were developed to represent the Flexible Semispan Model and the support mount for the FSM in the TDT. These finite element representations were independently correlated to static-load deflection data and Ground Vibration Test (GVT) data of the model and mount. These correlated FEMs were then used as the FSM structural representation for static and dynamic (flutter) aeroelastic analyses.

The MSC/NASTRAN finite element model and the corresponding doublet-lattice aerodynamic model used in the linear flutter analysis are shown in Figure 8. The finite element model has approximately 400 nodes, and the doublet-lattice model has 420 boxes (21 strips of 20 boxes each). The CFL3D.AE-BA aerodynamic mesh is shown in Figure 9. This finite-difference grid is a single block, C-O topology mesh with dimensions of 241 (chordwise) x 65 (spanwise) x 49 (normal) for a total of roughly 750,000 grid points. Clustering was suitable for inviscid (Euler) analysis.

A separate FEM of the FSM was constructed at Boeing Seattle for use in the Elfini analysis system. This 2595-node model is shown in Figure 10. This "enhanced"

model was constructed to gain familiarization with the structural idealization of the FSM and to improve upon, for correlation purposes, the finite element discretization and modeling of the original NASA/LMES model.

Static Aeroelastic Correlation

Static aeroelastic results were calculated using several approaches. The first approach used an ELFINI correlated FEM and produced results for two separate but similar aeroelastic analyses. This approach combined either PANAIR or TRANAIR (BL) aerodynamics with an ELFINI Aeroelasticity analysis. A second approach used a correlated NASTRAN FEM coupled with a doublet lattice method (DLM/ZONA - Linear Theory). The final approach used the correlated NASTRAN FEM to provide a structural model in the form of generalized mass, damping, and stiffness for a CFL3D-AE-BA analysis. This approach used CFL3D Euler aerodynamics coupled with the structural equations to predict the static-aeroelastic equilibrium solution. Overall, the results were encouraging - there was good correlation with wing force and moment data, and pressure data, at subsonic and supersonic conditions, but the correlation was not completely satisfactory because of discrepancies with measured wing twist and deflection data. A correlation of the wing lift-curve slope for a variation of Mach number is shown in Figure 11. This figure shows reasonably good correlation of the wing lift-curve results for all the analyses at subsonic conditions (Mach 0.80). Again at Mach 0.95, the correlation declines except for PANAIR/ELFINI for which it should be noted as an anomaly based on the correlation with measured sectional pressures.

Dynamic Aeroelastic Correlation

Three approaches were used for the flutter correlation. First, a linear flutter analysis was performed using the MSC/NASTRAN finite element model with doublet lattice aerodynamics. Second, the modal structural dynamic model was input into CFL3D.AE-BA and time-marching aeroelastic simulations were performed to investigate the flutter behavior with nonlinear aerodynamics. Third, a linear flutter analysis was performed using the ELFINI correlated FEM with ELFINI SINGULARITY doublet lattice aerodynamics.

Flutter analysis produced somewhat encouraging correlation with the limited flutter data for the FSM, in spite of uncertainties in the test configuration. A linear flutter analysis for the FSM, based upon a correlated FEM and modal frequencies - measured just prior to model loss, is shown in Figure 12. There are two distinct flutter mechanisms in the analysis: A "hard" flutter mode with a well-defined flutter boundary that correlates reasonably well with the measured "hard" flutter points, and a "hump" flutter mode with an ill-defined boundary that shows an instability over a large range of Mach/Q conditions.

Flutter mechanisms that show the "hump" behavior illustrated in Figure 12 are very sensitive to small changes in structural and aerodynamic modeling, and are very difficult to predict analytically. The conjecture (which has been validated to some extent by aeroelastic CFD analysis) is that the "hump" mode is, in reality, slightly stable in general, but that transonic interactions near Mach 1.0 cause a decrease in damping. This destabilizes the hump mode over a large range of dynamic pressures between Mach 0.98 and 1.0, resulting in the "chimney" of high dynamic response seen in the experimental results.

In order to further investigate the flutter behavior of the FSM in the high transonic regime, a series of nonlinear flutter analyses were performed using the CFL3D.AE-BA code. Time domain flutter simulations were performed at conditions ranging from Mach 0.8 to Mach 1.02, and dynamic pressures from 150 PSF to 300 PSF.

The nonlinear flutter results are summarized in Figure 13. In this plot, all CFD simulations are shown. The symbol is a square if the simulation showed no instabilities, and a triangle if an instability was found. The resulting flutter stability boundary is also plotted. Good correlation was obtained between the hard flutter boundary from CFL3D.AE-BA and the experimental hard flutter points. In addition, CFL3D simulations showed a second instability with a frequency consistent with the high dynamic response between Mach 0.98 and 1.00.

Overall, the FSM provided a fair amount of static aeroelastic data, but not as much dynamic aeroelastic flutter data as expected. A well defined model and flutter boundary (from Mach 0.70 to 1.15) is necessary to further assess the codes. Future testing of the ASE wind-tunnel models should provide the required aeroelastic data.

References

12. Technical Milestone Report, "Flexible Semispan Model (FSM) Analysis-Test Correlation," CRAD-9408-TR-3342 dated September 29, 1997.

13. Technical Milestone Report, "Analysis-Test Correlation of the HSR Flexible Semispan Model," DTF 26-2-02 dated November 12, 1997.

14. Baker, Mendoza, and Hartwich, " Transonic Aeroelastic Analysis of a High Speed Transport Wind Tunnel Model," AIAA 99-1217, 40th AIAA/ASME/ASCE/AHS/ASC Structures, Structural Dynamics, and Materials Conference, St. Louis, MO, April 1999.

FEM
622 Elements
399 Nodes
798 Degrees of Freedom

Doublet-Lattice Model

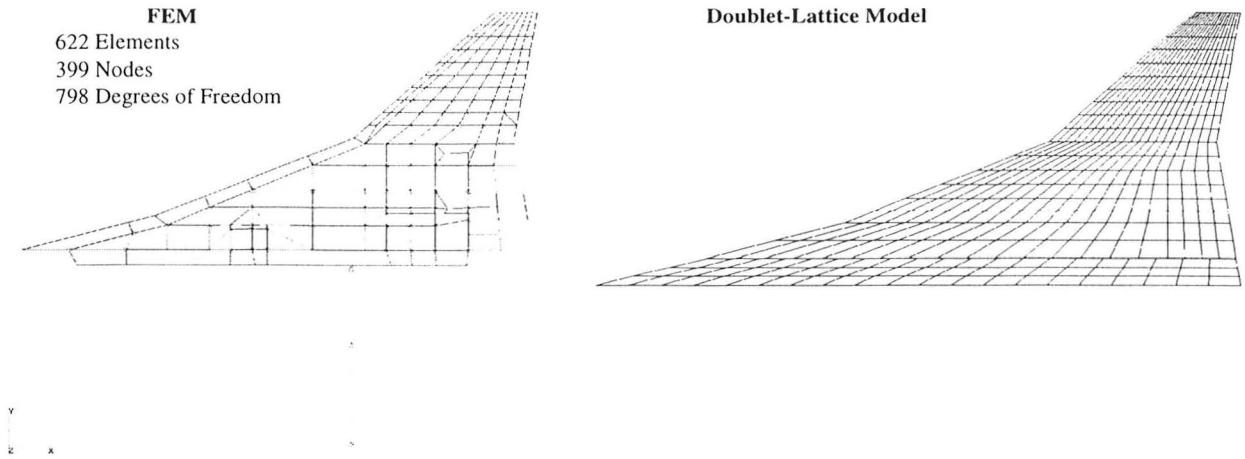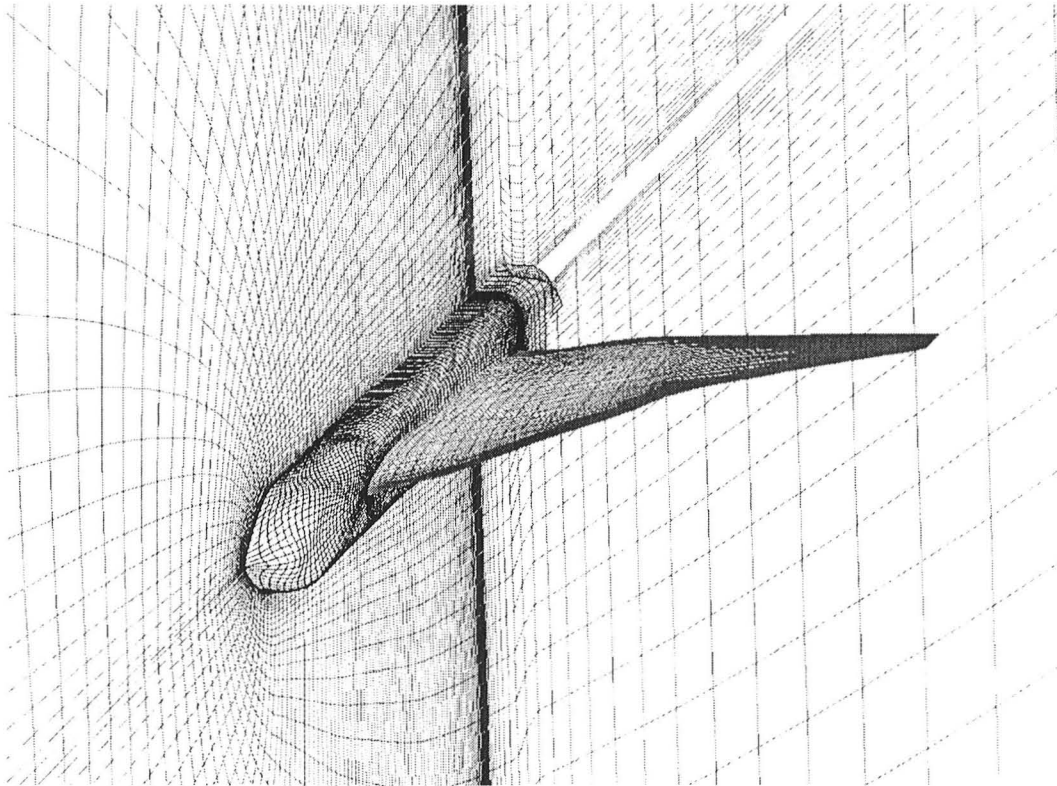Figure 8 NASTRAN Finite Element and Doublet Lattice Models.

Figure 9 Euler CFL3D-AE.BA Mesh Used in Nonlinear Aeroelastic Analyses.
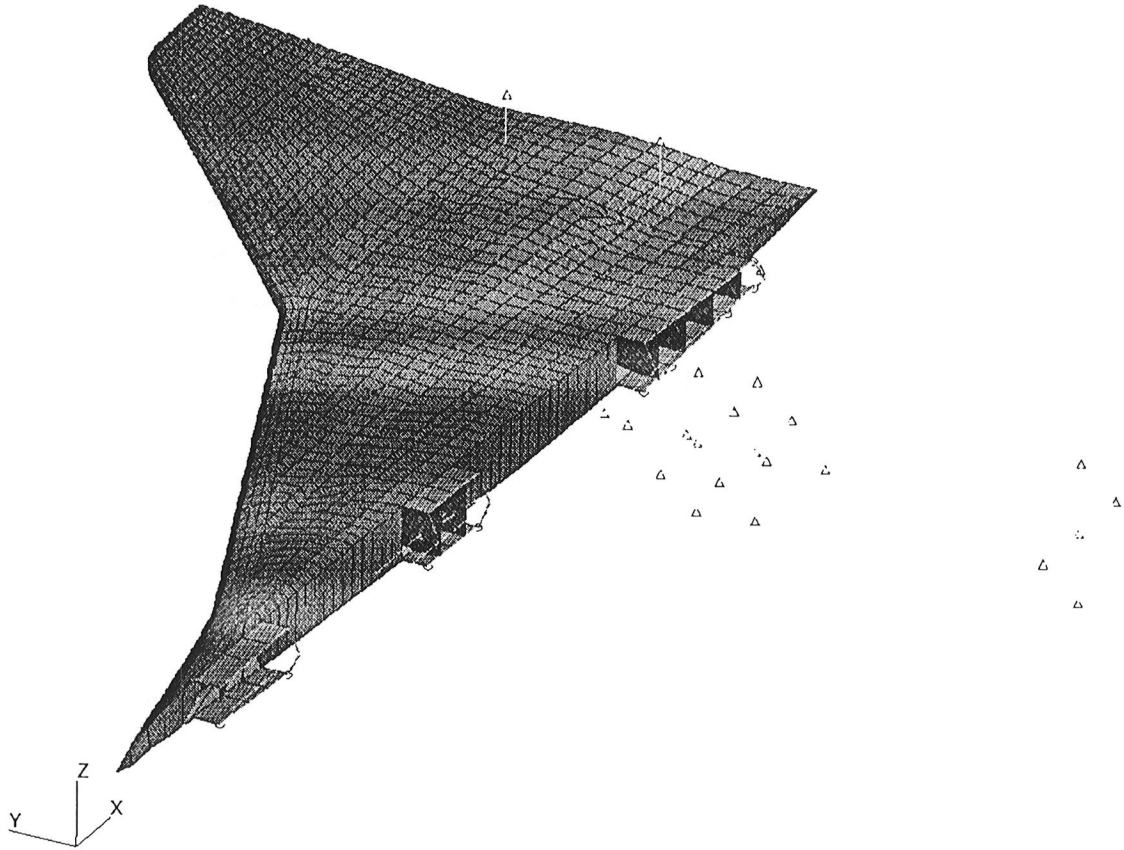
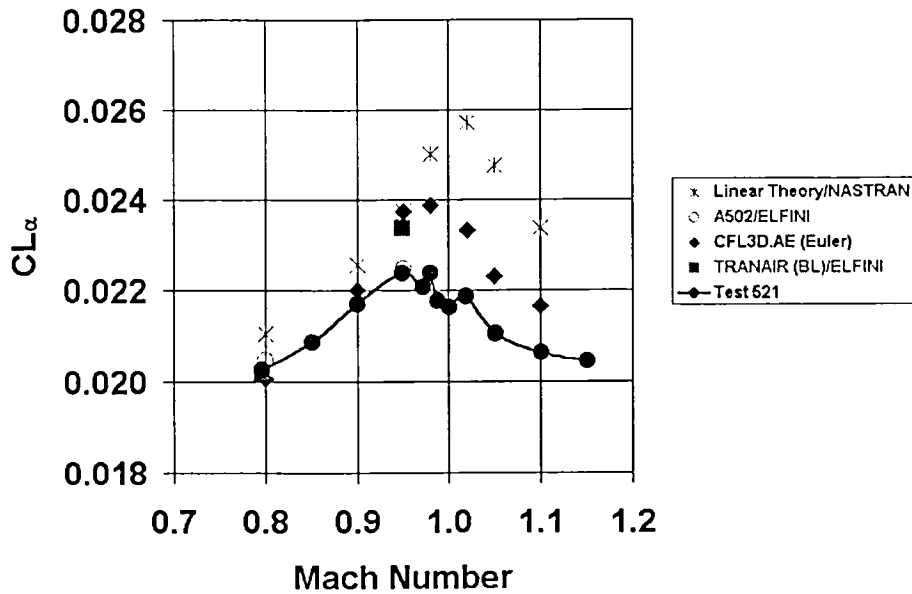Figure 10 "Enhanced" Elfini finite element model of the FSM.

Figure 11 Variation of computed and measured lift-curve slope with Mach number for the FSM (clean wing configuration).
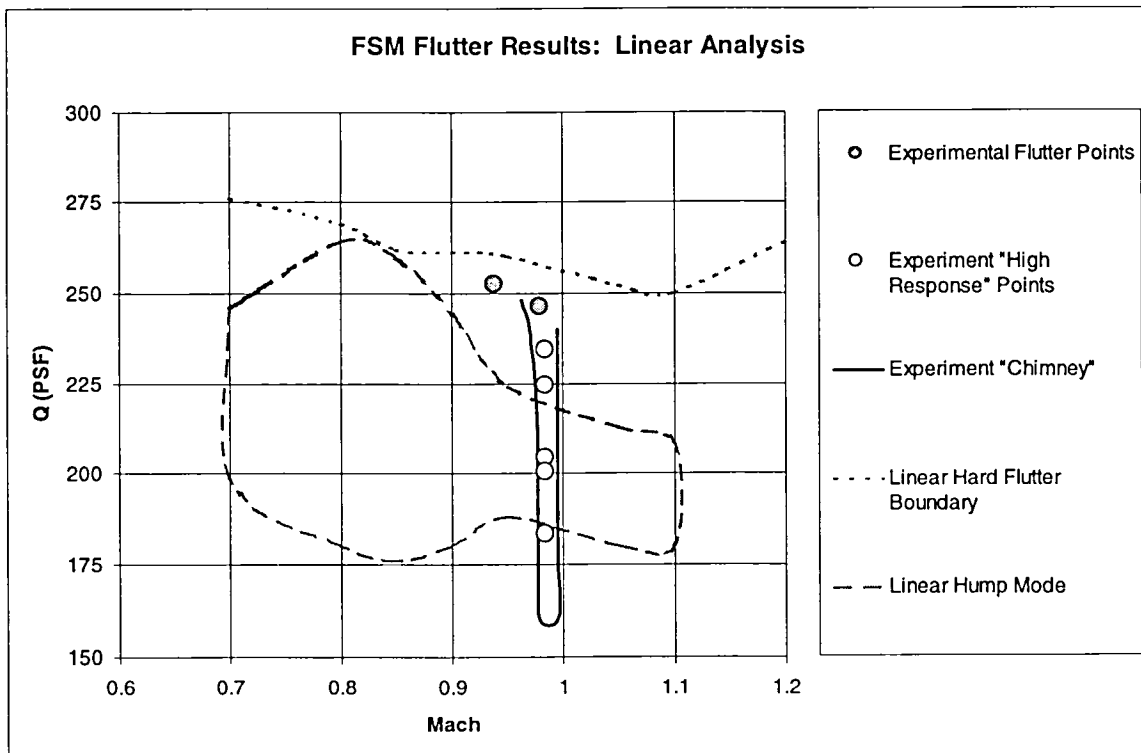
Figure 12 Linear flutter boundary using measured modal frequencies prior to model loss.
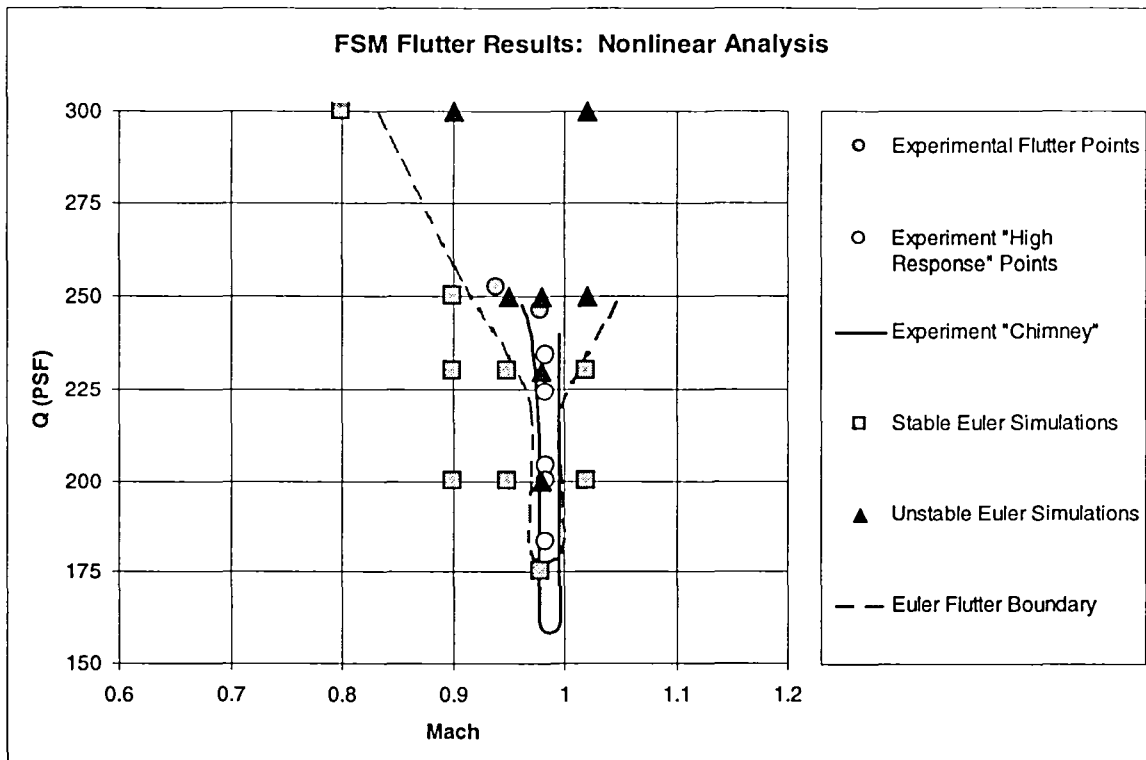
Figure 13   Nonlinear flutter boundary using CFL3D Euler aerodynamics.

4.1.3 Investigation of wall interference in the NASA TDT

Testing of the RSM in the TDT demonstrated a strong influence of the configuration (open or closed) of the tunnel wall slots on the model test data. In support of the Code Assessment I milestone, the objective of this subtask was to investigate the wall interference effects in the TDT with emphasis on how best to configure the tunnel for the ASE models tests. The report in Reference 15 was issued as the contract deliverable.

The objectives of this investigation were to: (1) develop a CFD model of the slotted-wall test section of the Langley Transonic Dynamics Tunnel, (2) perform steady-flow analysis of the HSR Rigid Semispan Model in the tunnel, at tunnel test conditions, to investigate tunnel wall and slot effects, (3) compare results with TDT520 test data, (4) assess blockage and lift interference, (5) assess a need for further investigation. The approach taken was to use TRANAIR, a Boeing developed transonic full potential flow solver with viscous boundary layer coupling, to investigate wall interference (lift and blockage interference) in the TDT for the RSM. A CFD model of the wind tunnel test configuration was developed for TRANAIR, illustrated in Figure 14. The model included the RSM configuration and the TDT test section walls with discrete contoured slots on the floor, ceiling, and sidewalls.

Parametric CFD studies were performed for various wind tunnel wall configurations: (a) East wall slots closed, (b) "free-air" condition - no tunnel walls, (c) all tunnel slots open, and (d) all tunnel slots closed. Flow analyses were performed at Mach 0.80, 0.95, and 1.15 at 0 and 2 degrees angle of attack. Preliminary results indicate that the walls and slots modify the flow field experienced by the model by changing the velocity magnitude and direction to values different from what the "free-air" model will experience.

Calculated results for the East wall slots open and closed predicted wing-load trends that were similar to those observed during TDT Test 520 of the RSM. Wall interference estimates for the East wall slots closed indicate that lift interference is small at Mach 0.80 and 0.95, but blockage interference may be significant at Mach 0.95 due to the relatively long body fairing of the RSM.

Recommendations include (1) further calibration of the TRANAIR TDT model based on measured wall pressure and balance data from a TDT static model test and (2) further studies to assess wall interference on dynamic model data to better understand these effects on flutter testing. Both recommendations assume continued efforts by NASA to calibrate the TDT. Results of the tunnel calibration effort will provide further insight into TDT wall interference effects as well as improve the overall understanding of the TDT flow quality.

References

15. Technical Milestone Report, "Preliminary Wall Interference Assessment For NASA Langley Transonic Dynamics Tunnel," DTF 26-3-07 dated October 30, 1998.
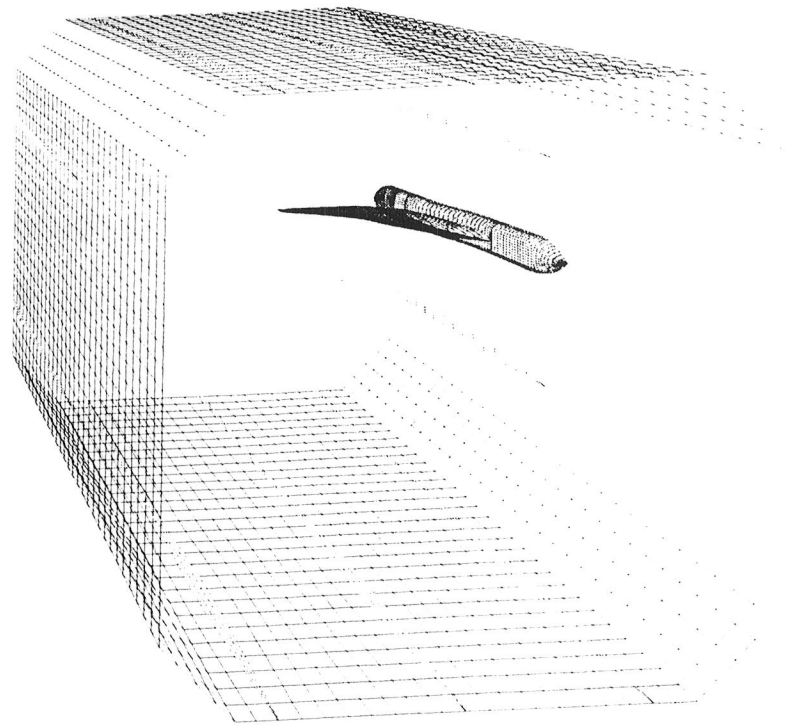
Figure 14 Iso-parametric view of the grid panel networks for the RSM and the TDT test section.

4.2 Code Assessment II

Available results from the RSM PAPA and the RSM OTT tests were to be added to the test data used for the previous Code Assessment I so that an updated code assessment could be made. Only the RSM PAPA results were available as new test data for this level 3 milestone.

4.2.1 RSM PAPA analysis/test correlation

Work performed by Boeing Long Beach

During the RSM/PAPA test, NASA performed several measurements to determine the structural properties of the RSM/PAPA configuration. These measurements included mass properties measurements, static stiffness measurements, ground vibration test (GVT) measurements, and flutter tests. NASA also developed a two degree of freedom structural dynamic model based on the measured mass and stiffness properties. While this model accurately captured the mass and stiffness properties of the RSM/PAPA, there were significant discrepancies between the frequencies and mode shapes predicted by this model and those measured in the GVT. The discrepancies were much greater when a flutter analysis was performed

with this preliminary structural model, and it was determined that changes would be required to improve correlation with the measured dynamic properties of the RSM/PAPA.

The results of this correlation are shown in Figure 15 and Tables 2 through 4. Figure 15 shows the experimentally determined vibration mode shapes for the RSM/PAPA with no ballast. The symbols show the measured mode shape values at each of the accelerometer locations, and the lines represent a least squares linear fit to the accelerometer data. Since the model was rigid except for pitch and plunge springs, the straight-line behavior was expected. Table 2 shows the frequency and mode shape comparison between the original structural model and the GVT results. In this table, the mode shape is quantified in terms of the rotation-to-translation ratio (R/T). Note that there are significant differences between the experimental and analytical frequency and mode shape results.
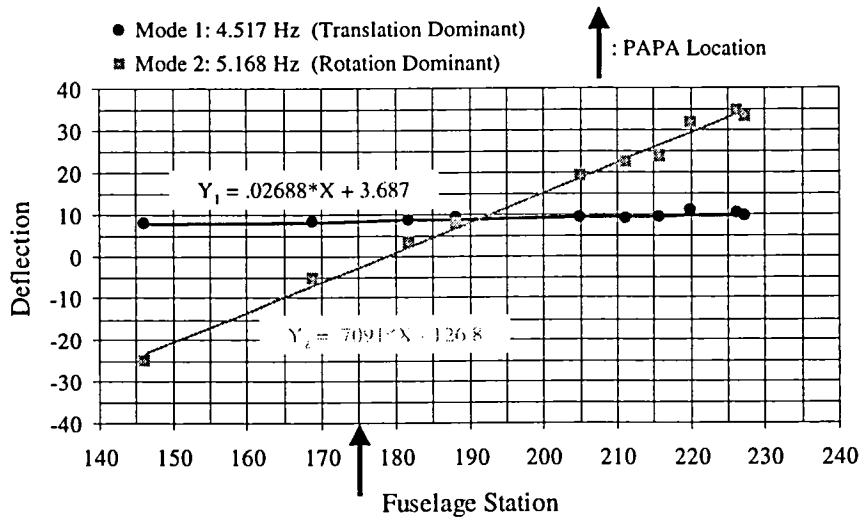
Figure 15 Fit GVT mode shapes using linear least squares method.

Table 2 Comparisons of GVT and analytical modes

	Mode 1		Mode 2	
	Frequency, Hz	Mode Shape, R/T	Frequency, Hz	Mode Shape, R/T
GVT	4.517	-.0032	5.168	.2842
Initial Model	4.802	.0019	5.371	-.6355
Updated Model	4.517	-.0041	5.166	.2862

R/T: Rotation Motion divided by Translation Motion

In order to improve correlation with the test data, an in-house FEM tuning process was used (Reference 16). In this process, the structural properties were modified to match the experimental frequencies and vibration mode shapes while attempting to minimize changes to the overall mass properties (weight and moment of inertia) of

the model. The vibration results are shown in Table 2, and it is clear that the updated model gives very good correlation with the GVT results. The modifications that were made to the structural model are summarized in Table 3. Note that minimal changes were made to the overall mass properties. The CG position was shifted by approximately one inch, and the spring rates were reduced by approximately 10%.

Table 3 Two degrees of freedom structure model

	Weight (lbs)	Inertia (lb-in^2)	Mass Unbalance (inch)	Spring (T) (lbs/in)	Spring (R) (lb-in/rad)
Initial Model	441.2	285800.	-.3152	1040.	842000.
Updated Model	439.2	285800.	.8142	918.6	776800.

T: Translation   R: Rotation

Since GVT data was available for several ballast conditions, a vibration analysis was performed using the original and the updated models for each of the ballast conditions, and the results are summarized in Table 4. Note that there is improved correlation across the board, with the maximum frequency error decreasing from 6.5% to 2% for any of the ballast configurations. A flutter anlaysis was also performed with this updated structural model, and the correlation was not as good as expected.

Table 4 Natural frequencies of clean wing with different ballast masses

Ballast Mass (lbs.)	C.G. Offset (inch)	Mode 1, Hz			Mode 2, Hz		
		GVT	Initial	Updated	GVT	Initial	Updated
0.0	.8140	4.517	4.802(6.3)	4.517(.00)	5.168	5.371(3.9)	5.166(.04)
5.1	1.466	4.563	4.773(4.6)	4.471(2.0)	5.000	5.220(4.4)	5.048(.96)
6.9	1.693	4.500	4.760(5.8)	4.452(1.1)	4.938	5.174(4.8)	5.013(1.5)
10.0	2.079	4.469	4.730(5.8)	4.414(1.2)	4.875	5.107(4.8)	4.961(1.8)
15.1	2.702	4.375	4.661(6.5)	4.342(.75)	4.875	5.028(3.1)	4.896(.43)
19.4	3.217	4.313	4.587(6.4)	4.275(.88)	4.875	4.986(2.3)	4.856(.39)

Numbers in parenthesis is the percentage error.

Once the structural model was correlated with the GVT data, the focus was shifted to the aerodynamic model to resolve the remaining discrepancies. A comparison between the MSC/NASTRAN doublet-lattice aerodynamics and the measured aerodynamics in the TDT revealed that the aerodynamic center predicted by NASTRAN was 3.188 inches aft of that measured in the TDT. This analysis was performed at Mach 0.7. In order to improve agreement between the NASTRAN analysis and the test, the geometry of the aerodynamic model was modified to place the aerodynamic center at the measured AC position. Once that modification was completed, flutter correlation was substantially improved.

The first set of flutter analyses were run to determine the sensitivity of the flutter dynamic pressure to ballast mass. These analyses were performed at Mach 0.6 in

order to correlate with test data taken in the TDT. The results are shown in Figure 16, along with the geometry of the aerodynamic model. All the flutter boundaries vs. ballast mass are qualitatively similar. In all cases, there is no flutter below a critical amount of ballast. The flutter dynamic pressure then rapidly decreases with increased ballast mass to a minimum value of approximately 30 PSF. The correlation with the test data is dramatically improved with the updated structural and aerodynamic models.
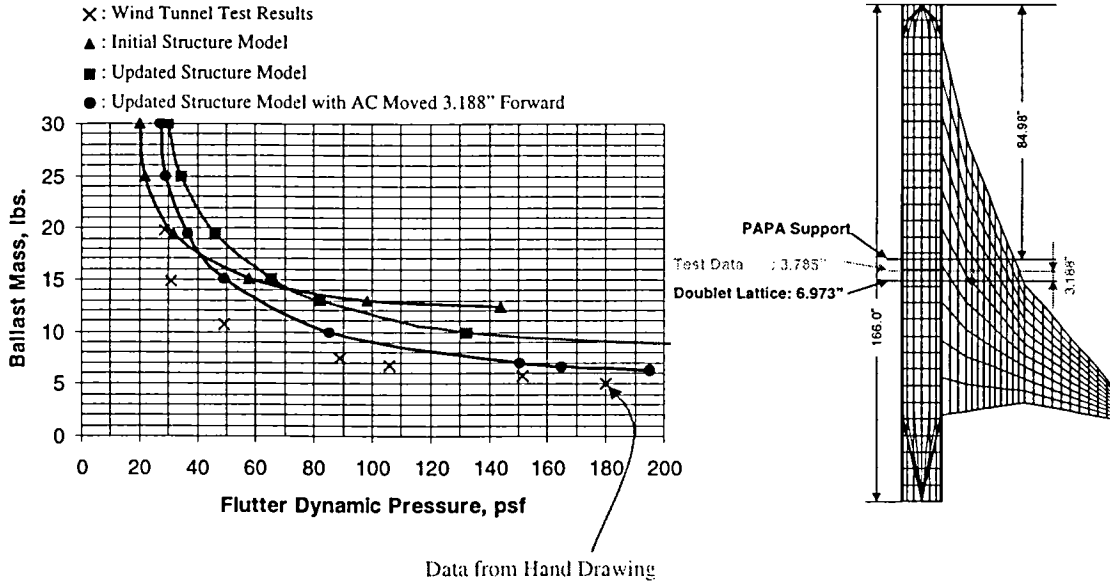

Figure 16 Flutter boundaries based on different aerodynamic center locations.

A flutter analysis was also performed to determine the boundary of flutter dynamic pressure vs. Mach number for a ballast mass of 6.9 lbs. The results are summarized in Figure 17. Note that for the original model, no flutter was found for this configuration. Correlation between the updated model and the experimental data is marginal, with a significant difference between predicted and measured flutter dynamic pressure. In addition, the analysis fails to predict the abrupt rise in flutter dynamic pressure at Mach 0.90. These discrepancies appear large, but their importance should not be overstated. It is clear from Figure 16 that, for 6.9 lbs ballast, the flutter dynamic pressure is extremely sensitive to small variations in ballast mass. This indicates that for this condition, the RSM/PAPA configuration is extremely sensitive to small variations in properties, and the small uncertainties in the structural model could easily cause a significant change in flutter dynamic pressure.

It is also interesting to note the strong dependence of the PAPA flutter boundaries on the aerodynamic center position. During the TDT test, it was observed that the flutter Q of the RSM/PAPA was very sensitive to small changes in angle of attack. It is speculated that leading edge separation (particularly on the lower surface of the outboard wing panel) is changing the effective aerodynamic center position as the

---

angle of attack is changed, possibly resulting in the large changes in flutter dynamic pressure.

X : Wind Tunnel Test Results
▲ : Initial Structure Model, NO FLUTTER
■ : Updated Structure Model, NO FLUTTER
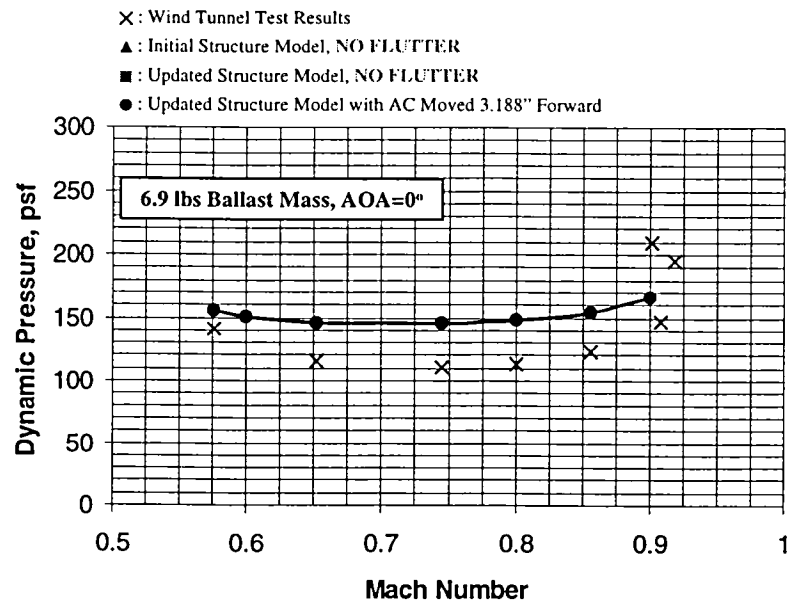● : Updated Structure Model with AC Moved 3.188" Forward

Figure 17 Flutter boundaries with 6.9 lbs. ballast.

In this Figure, flutter boundaries based on the updated structure model with center of pressure moved 2" forward are excellent agreement with the wind tunnel test data. However, flutter boundaries did not exist with the initial structure model.

In Figure 17, flutter boundary at Mach 0.6 with 6.9 lbs ballast is roughly 130 psf based on the linear interpolation. However, in Figure 16, flutter boundary under the same condition is 100 psf. Therefore, the wind tunnel data in Figure 16, obtained from the hand drawing, are not reliable.

Work performed by Boeing Seattle

An analysis of the High Speed Research (HSR) Rigid Semi-span Model (RSM) was performed for correlation with wind-tunnel test data from NASA Langley Transonic Dynamics Tunnel (TDT). The rigid wind-tunnel model was mounted on a flexible mount, called the Pitch and Plunge Apparatus (PAPA), which was designed to simulate a simple two-degree-of-freedom dynamic system. The primary purpose of the wind-tunnel test was to acquire unsteady pressure data, during two-degree-of-freedom flutter, to validate, calibrate, and correct linear unsteady computational procedures and codes; and to validate and enhance nonlinear computational methods and codes suitable for application to High Speed Civil Transport (HSCT)

The analysis of the RSM-PAPA wind-tunnel model was based upon a simple two-degree-of-freedom finite-element model. Dynamic characteristics of the model were assumed to be well defined for the two-degree-of-freedom system, since physical properties had been measured for the key quantities of the dynamic system. Physical properties incorporated into the finite element model were based upon these measured quantities.

A flutter analysis was performed, and results indicated that the initial baseline model was flutter-free for a Mach number range from 0.6 to 0.85, and for a dynamic pressure range from 0 to 300 *psf*. This result was counter to the observed flutter of the wind-tunnel model in the TDT. A free vibration analysis determined that the dynamic characteristics of the initial model did not correlate well with ground vibration data. Also, it was determined through further flutter analysis that significant changes to static unbalance were required to drive the analysis model to flutter. Tuning of the finite-element model was performed to correlate with ground vibration data. Although good correlation was achieved, the updated properties in the finite element model significantly deviated from measured quantities. A flutter analysis was performed using the updated model, but that too was found to be flutter-free across the Mach number range and dynamic pressure range investigated. Neither the initial or the updated finite-element model would flutter, even at low mach numbers, where linear aerodynamic models are believed to be adequate.

Additional investigation is required before the RSM-PAPA analysis / test correlation can come to a meaningful conclusion. The assumption that a simple two-degree-of-freedom finite-element model can accurately represent the dynamic characteristics of the RSM-PAPA should be investigated further, since the initial model, based upon measured physical properties, did not correlate well with GVT mode shapes. Further investigation should focus on the structural dynamic characteristics of the model before attempts are made to correlate with aeroelastic wind-tunnel data.

References

16. Chan-gi Pak, "Efficient Finite Element Model Correlation and Validation," MDC 96K7262, December 20, 1996.

4.2.2 RSM OTT analysis/test correlation

Work performed by Boeing Long Beach

An unsteady Euler analysis of the Rigid Semispan Model (RSM-OTT) was performed with the CFL3D.AE-BA code. The computed unsteady pressure results during the last cycle of sinusoidal pitching were post-processed using Fourier transformation to get magnitude and phase angle of $\Delta C_p / \Delta \alpha$.

Table 5 provides an overview of the Euler analysis for the RSM-OTT wing/body configuration.

Table 5 Summary of Analyses for RSM-OTT Wing/Body.

Case	Mach number (M)	Angle of attack (α)	Amplitude: Δα	Frequency (Hz)
Steady-state	0.8	-3°, 0°, 3°, 9°	0	0
Sinusoidal Pitching	0.8	-3°, 0°, 3°, 9°	±1.0°	5
Sinusoidal Pitching	0.8	-3° and 3°	±0.25°	10

The magnitude of $\Delta C_p/\Delta\alpha$ for the $\Delta\alpha = \pm 1.0°$ and $f = 5$ Hz case is relatively small at $\alpha = 3.0°$ except the region near the leading edge of the outboard wing. As the angle of attack is increased to 9°, a significant increase in magnitude occurs on the upper surface at the 60% of the semispan station. As the angle of attack is decreased to 0°, large increases in magnitude occurs on the lower surface near the leading edge near the 60% semispan station and mid-chord at 95% semispan station. As the angle of attack is further decreased to -3°, the location of the maximum C_p magnitude on the lower surface at the 60% semispan station moves further downstream and large variations in magnitude occurs near the leading edge of the lower surface at 10% and 30% semispan stations.

The phase shift angle for the $\Delta\alpha = \pm 1.0°$ and $f = 5$ Hz case gradually increases with chordwise distance at $\alpha = 3.0°$ except the region near the trailing edge of the wing. As the angle of attack is increased to 9°, a large variation in phase angle occurs on the lower surface at all the semispan stations. As the angle of attack is decreased to 0°, significant variations in phase angle occur on both the upper and lower surfaces near the wing tip region. As the angle of attack is further decreased to -3°, large variations in phase angle are observed near the leading edge and wing tip regions.

The variations of $\Delta C_p/\Delta\alpha$ magnitude with chordwise distance for the $\Delta\alpha = \pm 0.25°$ and $f = 10$ Hz cases show the same trend as those of the $\Delta\alpha = \pm 1.0°$ and $f = 5$ Hz cases, but magnitudes for the $\Delta\alpha = \pm 0.25°$ and $f = 10$ Hz cases are higher than those for the $\Delta\alpha = \pm 1.0°$ and $f = 5$ Hz cases. The phase angle variation with chordwise distance for the $\Delta\alpha = \pm 0.25°$ and $f = 10$ Hz cases shows the same trend as those of the $\Delta\alpha = \pm 1.0°$ and $f = 5$ Hz cases, but slopes for the $\Delta\alpha = \pm 0.25°$ and $f = 10$ Hz cases are steeper than those for the $\Delta\alpha = \pm 1.0°$ and $f = 5$ Hz cases due to the fact that the flow has less time to respond to changes in angle of attack at a higher frequency.

5. Nonlinear Flutter Analysis Methods

Under this subtask, nonlinear flutter analysis capability was developed and applied to the analysis of the wind tunnel models and the TCA configuration. The analysis capability consists of two main approaches. The first is a CFD based nonlinear analysis capability that can be used to analyze the most difficult cases encountered for free-flying aircraft. The second is an efficient, production-level flutter analysis and design process which uses nonlinear steady and unsteady wind tunnel or CFD data to correct or replace linear aerodynamics. These tools were applied in order to evaluate the importance of nonlinear aerodynamics in the significant flutter mechanisms, and to thereby reduce aeroelastic risk. Experience in these applications, along with prior applications, also uncovers process shortcomings, and appropriate modifications/improvements to the processes can thereby be made.

5.1 Euler and Euler/Navier Stokes CFD Methods

5.1.1 E/N-S code with a dynamic flap analysis capability

Work performed by Boeing Long Beach

Software enhancements were developed and validated to allow the analysis of static and dynamic flap deflections in the existing Euler/Navier-Stokes CFL3D analysis code. This was required to simulate the driving unsteady flow mechanism used in the wind tunnel tests. In addition, this capability makes it possible to perform nonlinear analysis of wing load alleviation and flutter suppression systems.

5.1.2 Antisymmetric E/N-S aeroelastic analysis capability

Work performed by Boeing Long Beach

Currently, there is no efficient method of computing nonlinear antisymmetric flutter. Tip-to-tip (full span) CFD models are prohibitive compared to half-span models (twice the memory and CPU time), so a technique has been developed for implementing an antisymmetric boundary condition for Euler/Navier-Stokes aeroelastic analysis in CFL3D. This technique is applicable to antisymmetric flutter analysis in CFL3D as well as the rapid calculation of nonlinear lateral/directional stability and control derivatives.

The basic assumption is that the flow at the symmetry plane can be linearized about the symmetric condition. The flow on the unmodeled side of the symmetry plane can then be estimated using linear aerodynamic theories, and the approximation should be valid for "mild" antisymmetries such as small sideslip angles, small roll rates, and

small structural displacements. This concept is analogous to the current capability of most potential flow codes to model symmetric and antisymmetric conditions. In the CFD solutions, however, there is always a symmetric component of the flow due to the basic geometry and angle of attack of the airplane. The antisymmetric boundary condition needs to be formulated in terms of an increment to this mean symmetric flow, which requires more bookkeeping than in a linear code. The antisymmetric boundary condition has been derived in terms of the contravariant velocities, and the process is outlined in Figure 18.

- **Symmetry BC Formulation (l=l1 plane):**

$$u_{-1} = u_1 - 2\,\xi_x U_1$$
$$v_{-1} = v_1 - 2\,\xi_y U_1$$
$$w_{-1} = w_1 - 2\,\xi_z U_1$$

where U_1 is the normalized contravariant velocity in the ξ direction and ξ_x, ξ_y, ξ_z are the metrics at the l=1 face

Antisymmetric equivalent (application of the small disturbance formulation to the contravariant velocities):

$$u_{-1} = 2\,u_{s1} - u_1 - 2\,\xi_x(2\,U_{S1} - U_1)$$
$$v_{-1} = 2\,v_{s1} - v_1 - 2\,\xi_y(2\,U_{S1} - U_1)$$
$$w_{-1} = 2\,w_{s1} - w_1 - 2\,\xi_z(2\,U_{S1} - U_1)$$

where the index S1 corresponds to the symmetric solution at the l=1 index

Assumes small antisymmetric motion about symmetry plane → Range of applicability under investigation

- **Numerical Simulation Procedure**
    1- Symmetric solution
    2- Memorize symmetry plane solution (restart)
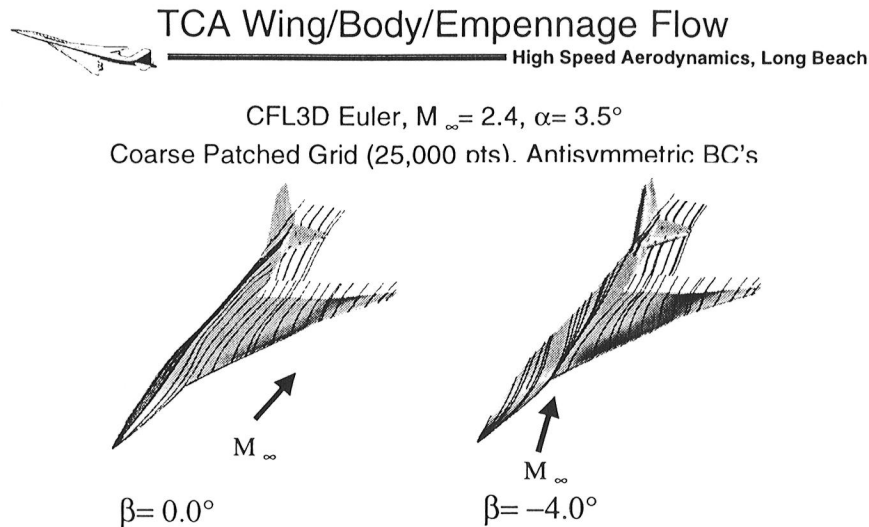   3- Run antisymmetric cases

Figure 18 Antisymmetric boundary condition formulation.

The numerical procedure by which "mildly" antisymmetric flows are to be computed is by computing the symmetric solution first. Once converged, the symmetric solution is "memorized" in the form of restart flow file for the 2 computational "symmetry" planes (+1 and 2 indices). This memorized flow field is then used to separate the CFL3D flow field into its symmetric and antisymmetric components, and the flow conditions in the ghost cells are then estimated.

Validation over simple geometries may not necessarily imply validity over realistic configurations. Therefore, it was decided that before undertaking an extensive validation study, one should test convergence with the new boundary conditions for a typical case involving an HSCT geometry with multiblock patched grids and flow non-linearities (shocks). As a result, a 7 block coarse wing/body/empennage TCA configuration with patched grids was used as a test case. The chart below shows the solutions obtained for both $\beta = 0°$ and $\beta = -4°$ on the TCA W/B/E configuration. The side slip case seems to display the expected flow features:

Stronger shocks (larger compressions) on the windward side of the wing since the flow component normal to the leading edge is larger.

Streamlines going through the symmetry plane.

A more quantitative validation of the antisymmetric boundary conditions has been performed using simpler CFD models. Specifically, the Benchmark Active Controls Technology (BACT) wing was modeled in half-span and full-span configurations. Both models were used to compute results for sideslip conditions and antisymmetric wing twist conditions. Comparisons of surface pressures, sectional loads, and streamlines for the half-span and full-span models showed excellent correlation for small antisymmetries.

TCA Wing/Body/Empennage Flow
High Speed Aerodynamics, Long Beach

CFL3D Euler, $M_\infty = 2.4$, $\alpha = 3.5°$
Coarse Patched Grid (25,000 pts), Antisymmetric BC's

M_∞

$\beta = 0.0°$

M_∞

$\beta = -4.0°$

BOEING

Figure 19 CFL3D antisymmetric boundary condition results for the TCA.

5.1.3 Time domain flutter identification techniques

Work performed by Boeing Long Beach

While there has been much recent progress in simulating nonlinear aeroelastic systems, and in predicting many of the aeroelastic phenomena of concern in transport aircraft design (i.e. transonic flutter buckets), the utility of a simulation in generating an understanding of the flutter behavior is limited. This is due in part to the high cost

of generating these simulations, and the implied limitation on the number of conditions that can be analyzed, but there are also some difficulties introduced by the very nature of a simulation. Flutter engineers have traditionally worked in the frequency domain, and are accustomed to describing the flutter behavior of an airplane in terms of its V-G and V-F (or Q-G and Q-F) plots and flutter mode shapes. While the V-G and V-F plots give information about how the dynamic response of an airplane changes as the airspeed is increased, the simulation only gives information about one isolated condition (Mach, airspeed, altitude, etc.). Therefore, where a traditional flutter analysis can let the engineer determine an airspeed at which an airplane becomes unstable, while a simulation only serves as a "binary check:" either the airplane is fluttering at this condition, or it is not.

In order to improve the utility of aeroelastic CFD solutions, a new technique was developed (the SYSID code) in which system identification is used to easily extract modal frequencies and damping ratios from simulation time histories, and shows how the identified parameters can be used to determine the variation in frequency and damping ratio as the airspeed is changed. This technique not only provides the flutter engineer with added insight into the aeroelastic behavior of the airplane, but it allows calculation of flutter mode shapes, and allows estimation of flutter boundaries while minimizing the number of simulations required.

The approach taken in the SYSID code is to assume that the dynamics of the aeroelastic system can be approximated by a linear state-space model of the same order as the purely structural dynamic system (wind-off). The state-space model is then estimated based on time history data from a fully coupled nonlinear aeroelastic CFD simulation (CFL3D.AE-BA). A representative application is shown in Figure 20. First, the time histories of two modal deflections are shown in Figure 20(a). It is clear that the dynamics of this aeroelastic system are quite complex, and that an "eyeball" estimation of stability is not reliable. Figure 20(b) shows the estimates of the frequency and damping of the aeroelastic system as the time simulation progresses (the estimates are updated at each iteration of the CFD solution). Note that good estimates of the frequency and damping are obtained after about 200 iterations. Finally, Figure 20(c) illustrates how the identified state-space models can be used to estimate the trends of frequency and damping as dynamic pressure is changed, which is extremely valuable for the flutter analyst.
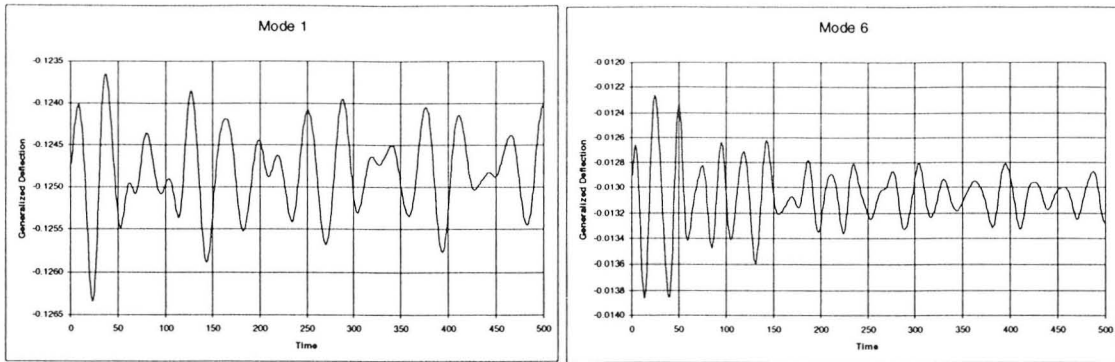
(a) Time histories of generalized (modal) deflections
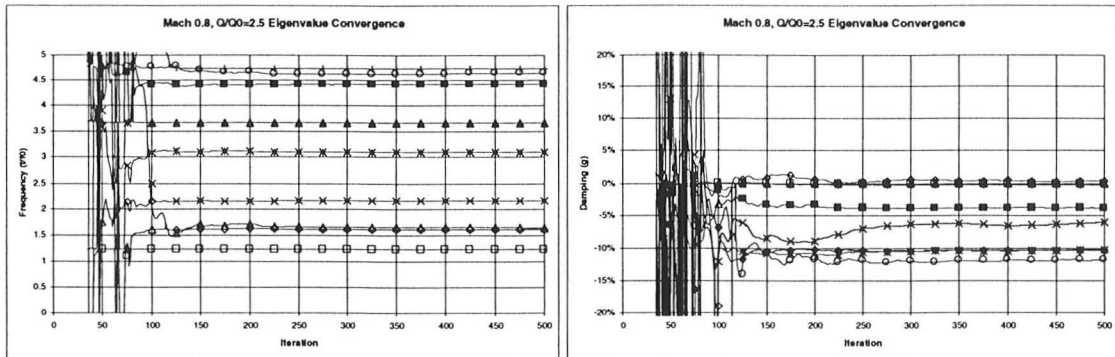
(b) Convergence of Eigenvalue Estimates from time history data
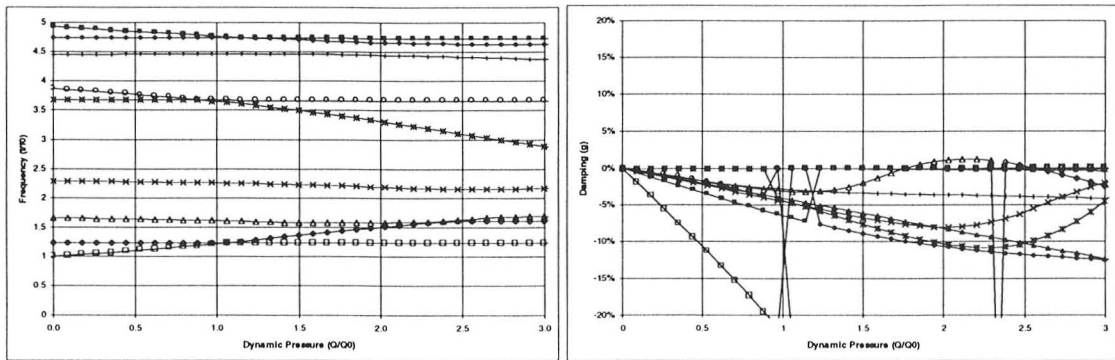
(c) Estimation of variation in frequency & damping with changes in dynamic pressure

Figure 20 Typical nonlinear flutter analysis results (Mach 0.80, Q/Q_0=2.5). Generalized deflection time histories from CFL3D.AE-BA, eigenvalue estimates from SYSID, and approximate Q-G/Q-F plots.

5.1.4 Evaluation of nonlinear effects on TCA flutter

Work performed by Boeing Long Beach

The baseline aircraft sized by the DITS Team used linear aerodynamic theory for the flutter analysis and design. This is the usual practice for most aircraft, however, nonlinear effects could be important for the HSCT. A verification of the flutter speed of the TCA baseline aircraft was performed using an aerodynamic theory that includes nonlinear effects determined using CFD data.

To this end, the performance of non-linear flutter calculations using time-marching Navier-Sokes solutions was necessary at two angles of attack: the first one being a case with attached flow (α=2.8°) and the second one being a leading-edge vortex dominated high alpha flow (α=12.11°). Static aeroelastic runs were converged and then used as a starting point for dynamic simulations. The Navier-Stokes analyses were conducted with the CFL3D.AE-BA code with the Baldwin-Lomax turbulence model. The Degani-Schiff option was turned on to improve the accuracy of the solutions at angles-of-attack where wing leading-edge vortices are expected to occur.

The CFL3D aeroelastic frequencies seem to correlate fairly well with linear analyses, while damping results vary significantly (especially for the low alpha case). The high angle-of-attack case does not show evidence of any new instabilities. It is possible that a leading-edge vortex induced instability might exist at other flight conditions, particularly at an intermediate angle-of-attack where the leading-edge vortex begins to form.

5.1.5 Evaluation of ENSAERO (canceled 9/96)

The ENSAERO Euler/Navier-Stokes CFD code was used for RSM analysis test correlation work by Northrop Grumman under subcontract to Boeing during the NAS1-20220 Task 17.1 contract, Reference 11, which was completed in December 1995. A review of funding and priorities led to cancellation of this effort from the Task 26 contract. No reportable results were obtained during Task 26.

References

11. NAS1-20220, Airframe Integration Task 17 (Aeroelasticity and Structural Dynamics Subtask 1) Final Report, dated March 31, 1996.

5.2 Nonlinear Corrections for Steady and Unsteady Aerodynamics

Work performed by Boeing Long Beach

One of the main shortcomings of CFD-based aeroelastic analysis is the large amount of computer CPU time required for the nonlinear time-domain simulations. Typically, the result of such a simulation would simply be estimates of the aeroelastic frequencies and dampings for the vehicle at a single point in the sky (mass case, mach, and dynamic pressure). In order to map out flutter stability boundaries for an airplane flutter clearance, a multitude of these simulations would be required. This is impractical in an industrial environment because the cycle time required for flutter analysis would be increased drastically over current flutter analysis methods such as the P-K method.

One way to take advantage of the improved accuracy of unsteady CFD codes while keeping analysis cycle time reasonable is to use the CFD data to apply corrections to a simpler (i.e. faster and cheaper) linear aerodynamic model. Since current production flutter analysis tools are based on frequency-domain Aerodynamic Influence Coefficient (AIC) matrices, the obvious approach is to use unsteady CFD data (typically in the time domain), transform it into the frequency domain, and use it to apply corrections to the linear frequency-domain AIC matrices computed from, for example, the doublet-lattice method.

A technique called Local Equivalence (Reference 17) has been used in the HSR Aeroelasticity task to develop frequency-domain corrected AIC matrices based on nonlinear aerodynamic data from Euler/Navier-Stokes simulations in CFL3D-AE.BA. The CORRECT program has been integrated into the aeroelastic solution sequences in MSC/NASTRAN, and the interfaces are documented in Reference 18. The resulting correction process has been used for both static (i.e. loads) and dynamic (i.e. flutter) analysis on several configurations ranging from wind tunnel models (the FSM, Reference 19) to full scale aircraft (the TCA, Reference 20). Additional applications (not funded under HSR) to the AGARD 445.6 wing using unsteady aerodynamics from CAP-TSD have also been performed, and are documented in Reference 21.

Some relevant results are shown in the following figures. Figure 21 shows a typical result for a steady condition. For this analysis, an aeroelastic analysis was performed at high angle of attack using linear (doublet-lattice) aerodynamics (diamonds) and in CFL3D.AE-BA (triangles). At this flight condition, there was a significant leading edge vortex, so the spanwise load distributions predicted by CFL3D and doublet-lattice were quite different. A third aeroelastic solution was the performed using doublet lattice aerodynamics corrected to match the steady (rigid) CFL3D results.

The resulting spanwise load distribution is shown by the third line (with X symbols), and is in much better agreement with the CFL3D results.

Figure 22 shows a typical unsteady result. The two halves of the figure show the real and imaginary part of the frequency-domain AIC matrix as would be used in a flutter analysis. The term plotted is the generalized aerodynamic force (GAF) in the first vibration mode due to a generalized deflection of the third vibration mode. As in the steady plot, the linear result, the direct CFD solution, and the result based on a corrected AIC matrix are shown. From this plot it is clear that the corrections bring the linear result into much closer agreement with the CFD solutions.

References

17. M. Baker, "Aerodynamic Correction Procedures for Linear Aerodynamic Methods," HSR Technical Report #CRAD-9408-TR-1046, March, 1996.

18. M. Baker, "Aerodynamic Correction Factors Applied to Static Loads and Flutter Analysis," HSR Technical Report #CRAD-9408-TR-2432, October, 1996.

19. M. Baker et. al., "Flexible Semispan Model (FSM) Analysis-Test Correlation," HSR Technical Report # CRAD-9408-TR-3342, September 1997.

20. M. Baker, K. Yuan, and P. Goggin, "Calculation of Corrections to Linear Aerodynamic Methods for Static and Dynamic Analysis and Design," AIAA-98-2072, 40th AIAA/ASME/ASCE/AHS Structures, Structural Dynamics, and Materials Conference, Long Beach, April 1998.

21. M. L. Baker, "CFD Based Corrections for Linear Aerodynamic Methods," 1997 AGARD Workshop on Numerical Unsteady Aerodynamics and Aeroelastic Simulation, Aalborg, Denmark, October 1997.

S panwis e L ift Dis tribution, HS CT 2.4-7A, M=0.6, Linear AOA=13 deg.
(All S olutions B as ed on S ame Deflected S hape and Have S ame T otal L ift)
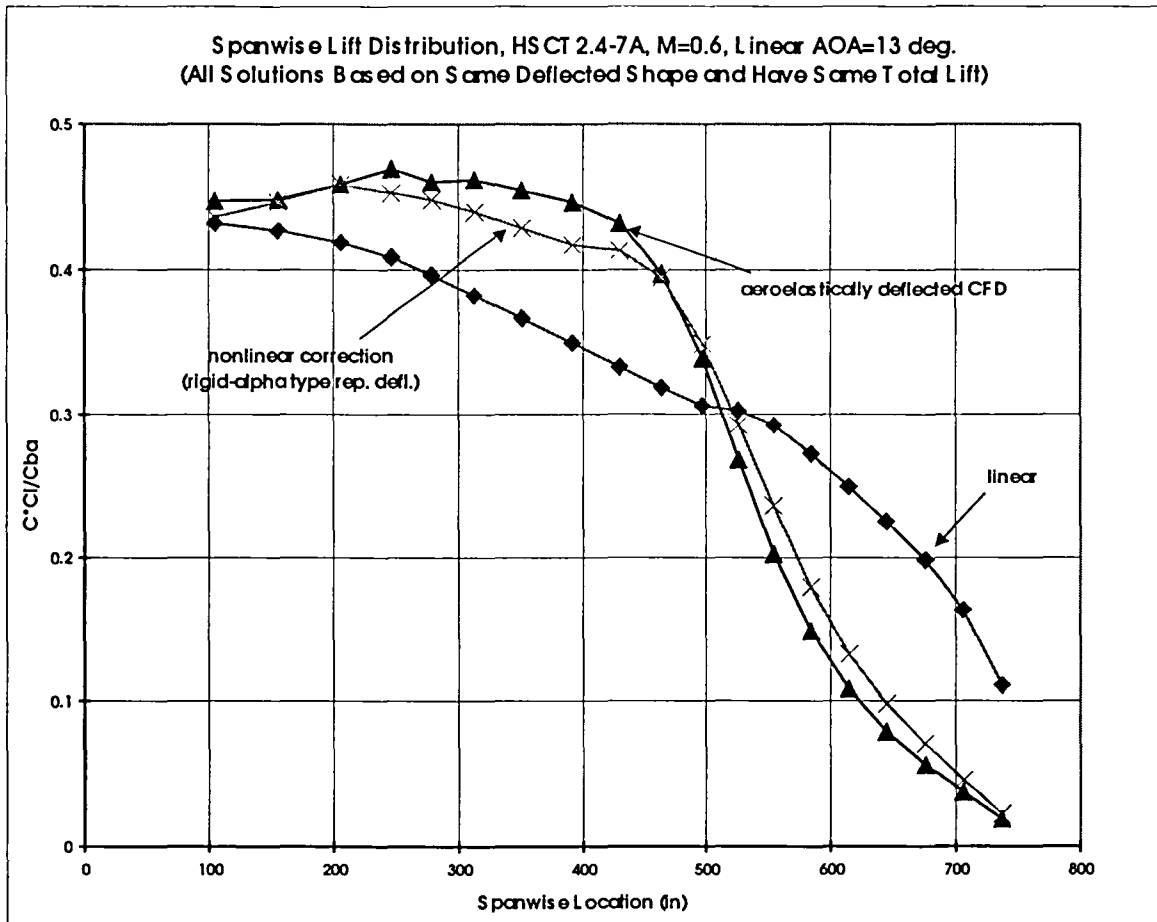

Figure 21 Wing Span Load Distribution Computed Using Linear Theory (Doublet-Lattice), CFD
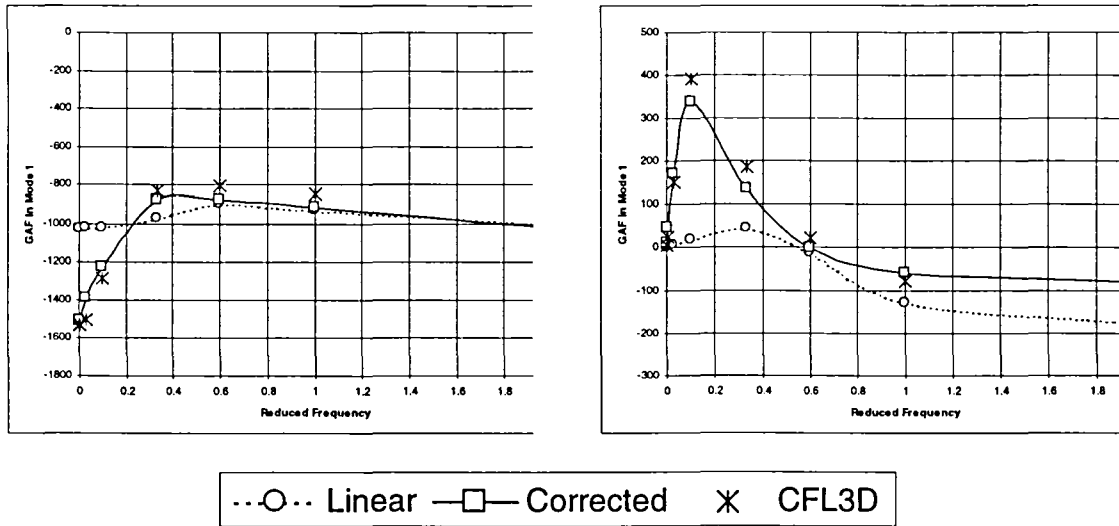(CFL3D-AE.BA), and Several Nonlinear Correction Processes.

··O·· Linear —□— Corrected ✕ CFL3D

Figure 22 Comparison Between Linear, Nonlinear, and Corrected Unsteady Aerodynamic Forces
(GAF in First Mode Due to Vibration in Third Mode).

5.3 TRANAIR Full Potential Aerodynamic Method

5.3.1 Application of TRANAIR to HSCT aeroelastic analysis

This subtask covered the implementation and assessment of the transonic full
potential code TRANAIR as an HSR analysis capability. Initial application of
TRANAIR to steady and unsteady HSCT aeroelastic applications was performed as
part of the RSM analysis test correlation effort reported in Reference 8. Fulfillment
of this contract deliverable requirement was also met by submittal of Reference 8.

References

8. Technical Milestone Report, "Correlation of A502 (PANAIR) and TRANAIR
Inviscid Results with NASA Langley TDT Test 520 Data for the HSR Rigid
Semi-Span Model," DTF 26-2-01 dated March 4, 1997.

6. Conclusions and Lessons Learned

- The wind-tunnel database that was acquired during the HSR Aeroelasticity Task did not completely fulfill the needs of the code assessment work.

  - There is a need for more static and dynamic aeroelastic data. The FSM provided a fair amount of static aeroelastic data, but very little dynamic aeroelastic flutter data. In addition the FSM flutter boundaries are questionable due to problems encountered during testing. A well defined model and flutter boundary (from Mach 0.70 to 1.15) is necessary. Tests of the ASM and AFM were originally to have helped fill this need.

  - The RSM flap data is a small limited set of unsteady data at Mach 0.80 for which the accuracy level is not known. Correlation of results with data shows that the codes predict the unsteady pressure magnitude higher than the measured data. Additional data of higher quality at transonic flow conditions is needed.

  - There is a need for well defined, controlled, unsteady aerodynamic wind tunnel model test data. Also, most data that has been acquired is for low reduced frequencies. The OTT test will provide additional and necessary data to assess unsteady pressure results assuming the OTT works and the RSM is "rigid". This data is very important since the model motion should be sufficiently measured (again assuming a rigid model).

  - Higher angle of attack data is desired to better understand nonlinear flow phenomena such as leading edge separation, but model and tunnel safety limitations may prevent the data from being obtained.

  - Need to thoroughly calibrate the TDT and evaluate wind-tunnel effects such as wall interference, blockage, up-flow angle, and side-flow angle. A detailed calibration of the flow in the tunnel test section would assist in resolving discrepancies between the test data and calculated results.

  - No data was obtained which included active flight control systems. The ASE models were to have provided this data.

  - No data for full span configurations was acquired. Effects of lateral motion and cable mounting to simulate free flight were not included. The RFM and AFM were to have provided this data.

- Lessons that were learned from the ASE models design effort:

  - There is a need from the outset for a thorough understanding of proposed materials. If there is not an existing material properties database, an appropriate and timely test plan should be conducted.

– FEM analysis based on proposed model concepts and designs is needed to guide the design process from beginning to end in a model design program. This analysis is required to verify that the design processes yield the target mass, stiffness, and structural dynamic properties. A plug-and-play approach in which model FEM components are combined with airplane FEM components (appropriately scaled) can provide piece-by-piece validation of the model design as it is completed. A final assessment must be made with a FEM of the model design in model scale.

Recommendations based on lessons learned

▪ Obtain a comprehensive set of unsteady pressure data (PAPA and OTT) that covers the transonic flow regime and includes practical angle of attack range – this is a missing element of our current test database.

● Build the analytical structural models (FEM) and correlate them with test data, including calibration data obtained for the installation in the wind tunnel. The correlation must occur as the calibration tests are being conducted.

● Develop a single validated finite-element model for each test and all aeroelastic correlation efforts should use the same model.

▪ With increased emphasis, undertake an analysis effort to predict the steady and unsteady flow characteristics as well as flutter characteristics, where applicable, of the planned test configurations before any testing. A certain degree of analysis-test correlation needs to occur while a test is still in progress to understand better the fidelity of the test data and to ensure that the required data has been collected.

▪ Strive to insure accurately measured displacements during testing (static and dynamic). Provide a data report describing test set-up and data reduction process. Provide an uncertainty analysis of the data. Improved reporting of the measured deflection data may provide a better understanding of the correlation.

▪ If feasible, use measured model geometry in future analysis/test correlation work. The current process for establishing wind tunnel model geometry needs to be improved to provide better surface definitions for CFD analysis.

▪ Support TDT calibration effort to define/understand data correction factors (for static pressure, total pressure, up-flow, lift induced up-wash, and blockage) which correct tunnel data (wall interference) to free-air data. Support uncertainty analysis effort to define/understand data uncertainty levels and biases. Both of these support efforts are key to improving the confidence level of the correction factors and the data.

▪ Develop model design and fabrication techniques to excite the model in a controlled, predetermined mode at varying frequencies in order to measure unsteady pressures corresponding to typical mode shapes. It may be feasible to obtain unsteady pressure

data at higher angles of attack than the current approach of oscillating a rigid model on the OTT.

Glossary

AFM	Aeroservoelastic Full Span Model
ASE	Aeroservoelasticity
ASM	Aeroelastic Semispan Model
BCAG	Boeing Commercial Airplane Group
BMT	Boeing Material Technology
BPW	Boeing Phantom Works
CDR	Critical Design Review
CFD	Computational Fluid Dynamics
DBT	Design Build Team
DITS	Design Integration Trade Study
DOF	Degree of Freedom
E/N-S	Euler/Navier-Stokes
FEM	Finite-element model
FSM	Flexible Semispan Model
GVT	Ground Vibration Test
HSCT	High Speed Civil Transport
HSR	High Speed Research
ITD	Integrated Technology Development
KEAS	knots equivalent airspeed
NDE	non-destructive evaluation
OTT	Oscillating Turntable
PAPA	Pitch and Plunge Apparatus
PCD	Planning and Control Document
PCD2	Planning and Control Document version revised 10/30/97
RCV	Ride Control Vane
RFM	Rigid Full Span Model
RSM	Rigid Semispan Model
TCA	Technology Concept Airplane configuration
TDT	Transonic Dynamics Tunnel
TMT	Technology Management Team

References

1. Schuster, D. M., Rausch, R. D.; "Transonic Dynamics Tunnel Force and Pressure Data Acquired on the HSR Rigid Semispan Model"; Aeroelasticity Section Report LMES ASR 96-07; December, 1996.

2. Schuster, D. M.; Spain, C. V.; Turnock, D. L.; Rausch, R. D.; Hamouda, M-N.; Volger, W. A.; Stockwell, A. E.; "Development, Analysis and Testing of the High Speed Research Flexible Semispan Model"; Aeroelasticity Section Report LMES ASR 97-01; February, 1997.

3. NAS1-20220, Annual Report for Calendar Year 1998, Work Performed Under Airframe Materials & Structures - 4.2, Aeroelasticity - 4.2.6.

4. Technical Milestone Report, "Flutter Sensitivity Study of the HSCT TCA Configuration as a Semispan Aeroelastic Wind Tunnel Model", DTF 26-1-07 dated November 5, 1997

5. Parametric Flutter Analyses of the TCA Configuration and Recommendation for FFM Design and Scaling", December 12, 1997.

6. Technical Milestone Report, "Code Assessment I Based on Baseline I Semispan Models Analysis/Test Correlation," dated March, 1998.

7. Technical Milestone Report, "Rigid Semispan Model (RSM) Analysis-Test Correlation," CRAD-9408-TR-2433 dated October 25, 1996.

8. Technical Milestone Report, "Correlation of A502 (PANAIR) and TRANAIR Inviscid Results with NASA Langley TDT Test 520 Data for the HSR Rigid Semi-Span Model," DTF 26-2-01 dated March 4, 1997.

9. Technical Milestone Report, "Rigid Semispan Model (RSM) with Flap Analysis-Test Correlation," CRAD-9408-TR-3691 dated September 15, 1997.

10. NAS1-20220, Annual Report for Calendar Year 1997, Work Performed Under Airframe Materials & Structures - 4.2, Aeroelasticity - 4.2.6.

11. NAS1-20220, Airframe Integration Task 17 (Aeroelasticity and Structural Dynamics Subtask 1) Final Report, dated March 31, 1996.

12. Technical Milestone Report, "Flexible Semispan Model (FSM) Analysis-Test Correlation," CRAD-9408-TR-3342 dated September 29, 1997.

13. Technical Milestone Report, "Analysis-Test Correlation of the HSR Flexible Semispan Model," DTF 26-2-02 dated November 12, 1997.

14. Baker, Mendoza, and Hartwich, " Transonic Aeroelastic Analysis of a High Speed Transport Wind Tunnel Model," AIAA 99-1217, 40th AIAA/ASME/ASCE/AHS/ASC Structures, Structural Dynamics, and Materials Conference, St. Louis, MO, April 1999.

15. Technical Milestone Report, "Preliminary Wall Interference Assessment For NASA Langley Transonic Dynamics Tunnel," DTF 26-3-07 dated October 30, 1998.

16. Chan-gi Pak, "Efficient Finite Element Model Correlation and Validation," MDC 96K7262, December 20, 1996.

17. M. Baker, "Aerodynamic Correction Procedures for Linear Aerodynamic Methods," HSR Technical Report #CRAD-9408-TR-1046, March, 1996.

18. M. Baker, "Aerodynamic Correction Factors Applied to Static Loads and Flutter Analysis," HSR Technical Report #CRAD-9408-TR-2432, October, 1996.

19. M. Baker et. al., "Flexible Semispan Model (FSM) Analysis-Test Correlation," HSR Technical Report # CRAD-9408-TR-3342, September 1997.

20. M. Baker, K. Yuan, and P. Goggin, "Calculation of Corrections to Linear Aerodynamic Methods for Static and Dynamic Analysis and Design," AIAA-98-2072, 40th AIAA/ASME/ASCE/AHS Structures, Structural Dynamics, and Materials Conference, Long Beach, April 1998.

21. M. L. Baker, "CFD Based Corrections for Linear Aerodynamic Methods," 1997 AGARD Workshop on Numerical Unsteady Aerodynamics and Aeroelastic Simulation, Aalborg, Denmark, October 1997.